10-11-2022

# Tuning the Structural Properties of Cellulose Acetate Thin Films: A Demonstration of Confinement and Antiplasticization in Cellulose Acetate Butyrate

Keegan Reece Parkhurst
*Rose-Hulman Institute of Technology*

# Tuning the Structural Properties of Cellulose Acetate Thin Films:

# A Demonstration of Confinement and Antiplasticization in Cellulose Acetate Butyrate

A Thesis

Submitted to the Faculty

Of

Rose-Hulman Institute of Technology

by

Keegan Reece Parkhurst

In Partial Fulfillment of the Requirements for the Degree

of

Master of Science in Chemical Engineering

October 2022

**ROSE-HULMAN INSTITUTE OF TECHNOLOGY**

**Final Examination Report**

**Keegan Parkhurst** — Name

**Chemical Engneering** — Graduate Major

Thesis Title **Tuning the Properties of Cellulose Acetate Thin Films: A Demonstration of Confinement and Antiplasticization in Cellulose Acetate Butyrate**

**DATE OF EXAM:** Otober 11, 2022

**EXAMINATION COMMITTEE:**

| | Thesis Advisory Committee | Department |
|---|---|---|
| Thesis Advisor: | Marissa Tousley | CHE |
| | Adam Nolte | CHE |
| | Michelle Marincel Payne | CE |
| | | |
| | | |

**PASSED** X **FAILED** _____

# ABSTRACT

Parkhurst, Keegan Reece

M.S.Ch.E.

Rose-Hulman Institute of Technology

October 2022

Tuning the Structural Properties of Cellulose Acetate Thin Films: A Demonstration of Confinement and Antiplasticization in Cellulose Acetate Butyrate

Thesis Advisor: Dr. Marissa Tousley

The development of high-performance cellulose acetate thin-film composite membranes will be essential to solving the growing water scarcity problems. To do this, understanding the fundamental structure of thin cellulosic films and its relation to transport is essential. In this work, thin cellulose acetate butyrate films were fabricated at varying thickness and treatments, such as soaking and plasticizer treatment. Their mechanical properties were analyzed using a surface wrinkling approach, and their hygroscopic properties were measured using swelling measurements and surface wrinkling under humid conditions. This work demonstrates confinement in cellulose acetate butyrate films at thicknesses below 45 to 70 nanometers. Plasticization is demonstrated in cellulose acetate butyrate film with an increase in swelling activity, but a decrease at low plasticizer concentration, indicating antiplasticization. There is a discussion on how these observations indicate changes in fundamental structural properties and can be used to predict transport properties.

Keywords: Thin-film composite membranes, cellulose acetate, confinement, antiplasticization, polymer structure

## DEDICATION

This work is dedicated to the support network around me during this project. This work is dedicated to the family, friends, and mentors that helped me get to this point. None of this could have been done without your support.

## ACKNOWLEDGMENTS

I acknowledge the contributions of many members of the Rose-Hulman academic community. I acknowledge the contributions of Frank Cunning as the laboratory technician for the laboratory where most of the research took place. I acknowledge the contributions of Brian Fair as the cleanroom facility manager and instrument technician of the M.I.N.D.s cleanroom. I acknowledge the contribution of Dr. Adam Nolte in helping to set up the humidity box for swelling and wrinkling measurements during humid summer months and his consults as an expert in the measurements used in this study.

## Table of Contents

## Table of Figures

## Table of Tables

**List of Symbols**

| | | |
|---|---|---|
| $\bar{E}_x$ | Plane-strain elastic modulus | Pa |
| $E_x$ | Elastic modulus | Pa |
| $\lambda$ | Wavelength | m |
| $h_f$ | Film thickness | m |
| $\nu$ | Poisson's ratio | unitless |
| $\phi_x$ | Thickness fraction | unitless |
| $S_h$ | Swelling ratio | unitless |
| $h_0$ | Film thickness (dry) | m |
| $d_t$ | Total film composite thickness | m |
| $\Delta\mu_s$ | Chemical potential gradient | J/mole |
| $G$ | Gibbs free energy | J |
| $n_s$ | Number of molecules | mole |
| $\rho$ | Frensel coefficient ratio | |
| $\Psi$ | Jones vector magnitude | radian |
| $\Delta$ | Jones vector phase shift | radian |
| $P$ | Force | kg m $s^{-2}$ |
| $\delta$ | Stroke | m |
| $R$ | Radius of probe | m |
| $d$ | Distance | m |
| $\theta$ | Angle | radian |

# 1. Introduction

## 1.1. Project Impact

The ability to supply society with adequate water for sanitation, drinking, and agriculture has been a focus of engineers since the beginning of the profession. In recent years, freshwater supplies have become increasingly strained in many populations, and there is a great amount of effort in determining how to meet these needs through other avenues [1]. These avenues include seawater and brackish water desalination and wastewater reclamation. Reverse osmosis is a process that is used in all of these applications [2] [3] [4]. Desalination by reverse osmosis is a mature technology with highly optimized membranes, the most dominant being the thin-film composite (TFC) membrane [5]. Developed in the 1980s, these membranes are aromatic polyamides formed through an interfacial polymerization process where polyamide is polymerized at the surface of the membrane, forming an incredibly thin layer that is selective to salt ions [5]. These membranes have been optimized to such a degree that systems can operate close to the thermodynamic limit of the separation. [6].

Despite TFCs' domination in the desalination market for the past 40 years, there are drawbacks to these membranes that become even more significant when applied to wastewater reclamation operations. One is their susceptibility to fouling from biological sources. Biofouling is when the surface of a membrane is damaged by the presence of microorganisms and natural organic matter produced by these microorganisms [7] [8]. This type of fouling occurs when microbes adhere to the surface of a membrane and form a biofilm [9] [10]. While there have been many innovations in the field of nanomaterials to mitigate biofouling, this phenomenon has made reverse osmosis almost impossible to be used effectively in wastewater treatment except in very specific feed streams [2]. The traditional solution to biological contaminants in a separation train is to use

disinfection processes, such as chlorination, to remove the bacteria before the reverse osmosis stage. TFC membranes are susceptible to chlorine, undergoing irreversible damage in the presence of parts-per-billion (ppb) levels of chlorine [2]. This issue significantly hinders the use of reverse osmosis in applications involving biological contaminants, such as wastewater reclamation, resource recovery, and bioreactors. This is unfortunate because reverse osmosis has a far superior capacity for removing many emerging contaminants than other technologies [11]. As such, there is a need to develop materials that can make reverse osmosis a more viable technology in these areas.

Cellulose acetate was the first material used for reverse osmosis and currently has niche applications due to a few of its properties. One is their resistance to biofouling. The smooth surface of the cellulose acetate membranes makes it more difficult for biofoulants to adhere and accumulate, making these membranes more stable long term in operations involving biofoulants . Another advantage is its resistance to chlorine. Unlike TFCs, cellulose acetate membranes can withstand 1 ppm of chlorine consistently [2]. This makes it significantly more effective in systems with disinfection steps.

Despite these advantages, cellulose acetate-based membranes suffer from low flux compared to polyamide TFC membranes. Cellulose acetate membranes are thicker than thin film composites, leading to lower water fluxes. This has led to cellulose acetate being confined to a minimal set of uses. Historically, there were attempts to create cellulosic thin film composites, but these membranes are difficult to fabricate without defects [12]. With the improvement and more widespread implementation of thin film fabrication technologies, there have been recent efforts towards developing cellulose acetate thin film composites for reverse osmosis, as well as thin cellulose acetate membranes for gas separations [13] [14]. These studies, along with investigations of other polymer systems in the membrane literature, have demonstrated a relationship between

membrane performance and polymer thin film structure and properties [14] [15] [16] [17]. There have been relatively few studies into cellulosic thin film composites for water purification operations. Therefore, a continued exploration into structure-property relationships in cellulose acetate-based films may help create more competitive cellulosic thin film composites and allow scientists and engineers to have better control over the transport properties of membranes for fine-tuning based on application.

### 1.2. Summary of Objectives

The primary objective of this work is to investigate the properties of cellulose acetate butyrate (CAB) thin films in response to confinement, changing humidity levels, and physical treatments known to cause changes to the polymer structure. Specifically, this thesis aims to:

1. Investigate the swelling behavior and elastic modulus of CAB thin films in the bulk (>100 nm) and confined (<40 nm) thickness regimes.
2. Explore the effects of physical treatments, such as water soaking and triacetin treatment, on CAB thin film swelling behavior and elastic modulus.
3. Investigate the effect of changing humidity levels on CAB film mechanical properties.

Through this exploration, this thesis aims to help contribute new knowledge for cellulose acetate-based thin films, specifically, and build on existing literature that has demonstrated connections between membrane transport phenomena and swelling behavior, mechanical properties, and plasticizer treatments for other polymer systems.

## 2. Background

### 2.1. Reverse Osmosis Membranes

The first materials used for high-performance reverse osmosis membranes were cellulose acetate and other cellulose esters [2]. These membranes were formed through the Loeb-Sourirajan process, where a casting solution is precipitated in a nonsolvent to form an anisotropic polymer film. The resulting membranes were thick, around 20 microns in thickness, and were anisotropic, with pore sizing increasing across the thickness of the membrane. Many different cellulose derivatives have been used for membranes, including cellulose acetate, cellulose acetate butyrate, cellulose acetate propionate, and cellulose triacetate, as shown in Figure 2.1. These cellulose esters are classified by the proportionate amount of acetyl, propionyl, and butyryl groups on the cellulose backbone. The cellulose chemistry plays a massive role in the resulting transport properties. For example, a study by Lonsdale et al. in 1965 showed that water permeation decreased with increasing acetyl content, but the salt selectivity increases [18]. Different esters and their casting solutions also have different morphological properties as well, as demonstrated by a study by Amim Jr. et al. [19]. In this study, the researchers demonstrated that cellulose acetate butyrate films spun in ethyl acetate and annealed exhibited root mean square roughness values around 0.3 nm. One recent study examined the effects of tuning the concentrations of different cellulose esters; CA, CAB, and CAP, on membrane performance. Cellulose acetate butyrate did not perform well by itself due to its hydrophobicity, but in blends with CA and CAP provided more stable rejection values at higher pressures, demonstrating the possible utility in using blends of different cellulose esters.

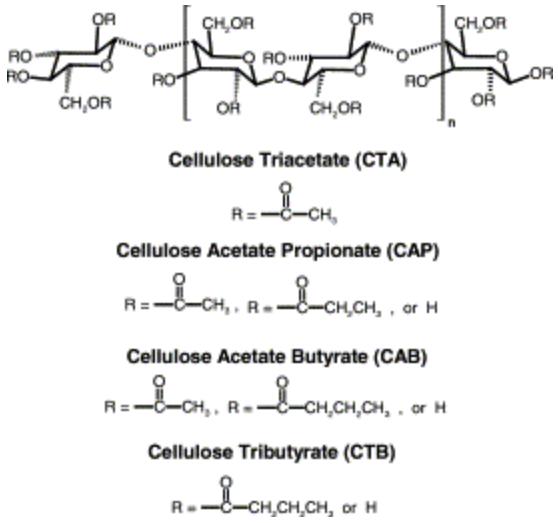


**Figure 2.1** - The general structure of cellulose-based polymers. Its classification is based on the content of acetyl and butyryl groups in the polymer. Reproduced from [20].

The most commonly used cellulose derivative for reverse osmosis is cellulose triacetate due to its very high selectivity [2]. These membranes dominated the reverse osmosis market in the 1960s and 70s due to their high selectivity and chemical stability. However, they are inherently limited in how much water they can filter due to their thickness. The Oak Ridge National Laboratory Office of Saline Water started pushing for the development of non-cellulosic membranes that could have a higher water permeability for nuclear applications, but other polymer systems could not compare to cellulose acetate membranes [2]. There were early attempts to develop cellulosic membranes thinner than possible with the Loeb-Sourirajan through an alternative fabrication technique, dip coating [12]. These membranes were difficult to fabricate due to the prevalence of minor defects destroying their performance. The process was much more expensive and difficult to scale up compared to phase-separation, so research focused on optimizing anisotropic thick cellulose acetate membranes rather than thin film-based membranes. Cellulose continued to dominate the reverse osmosis membrane market until the 1980s, when J.E.

Cadotte and his team at FilmTec pioneered an all-aromatic polyamide thin film composite membrane (TFC) called “FT-30” [21].

Polyamide TFC membranes are formed through an interfacial polymerization (IP) process, where membrane-forming monomers react at the surface of the membrane, allowing for the formation of an incredibly thin selective layer on top of the support layer. As can be seen in Figure 2.2, these membranes have significantly greater fluxes than cellulose acetate membranes, while maintaining high salt rejections. The IP process enabled the large-scale production of thin-film-based membranes, beating thick anisotropic membranes and the dominance of these membranes in the desalination market. Research in recent decades primarily focused on modifying the chemistry of the IP process to enhance flux and antifouling properties [22] [23].

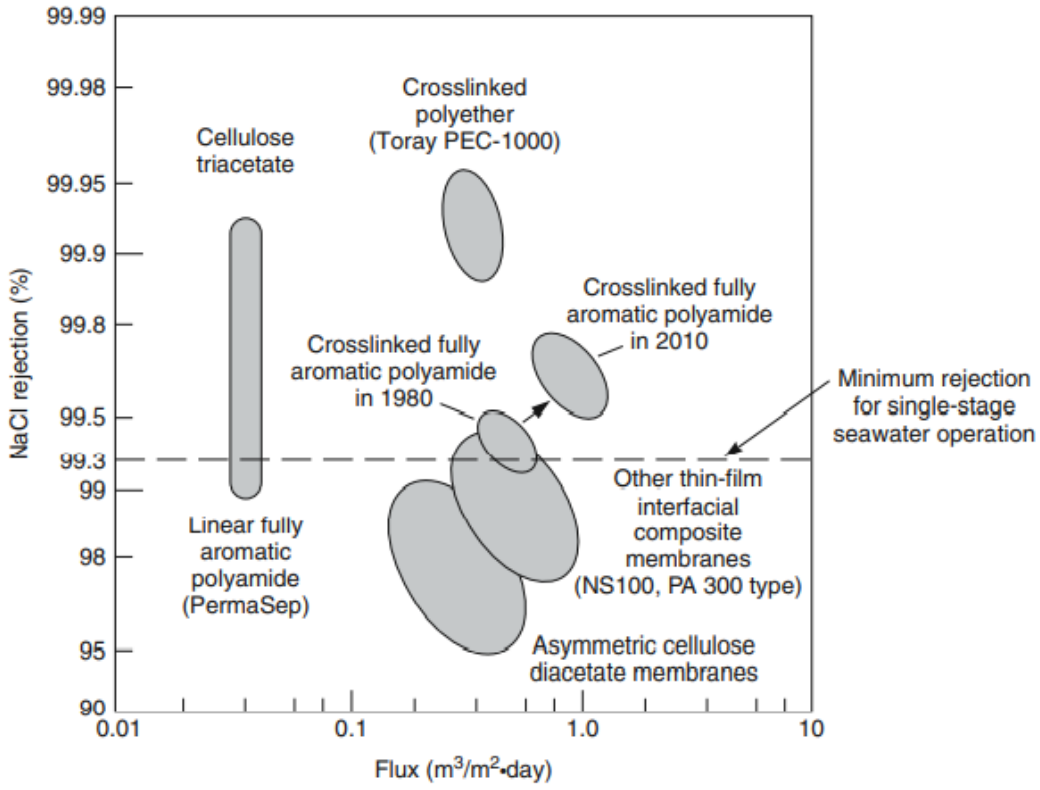


**Figure 2.2 -** Performance properties of membranes operating on seawater at 60 bar and 25° C. Reproduced from [2].

Despite the current widespread use of polyamide TFC membranes, these membranes do have downsides compared to cellulosic membranes, including their susceptibility to fouling, especially from biological sources [7] [8]. Fouling decreases the permeability of desalination membranes over time, which increases the energy requirements for desalination processes and introduces extra cleaning steps that cost resources, operation time, and energy [6] [2]. Cellulosic membranes are notably better at dealing with foulants such as natural organic matter. One study from Muna et al. recently compared cellulose triacetate (CTA) membranes and polyamide TFCs in a forward osmosis setup and found that while the TFC membrane had a much higher flux initially, it only took 5 hours for the TFC to have a lower flux than the CTA membrane [24]. The CTA membranes also showed a significantly higher flux recovery through cleaning. The study posited that the low surface roughness of CTA membranes led to their greater resistance to fouling. Another study by Zhang et al. in 2017 showed similar results comparing CTA and TFC membranes in an osmotic membrane bioreactor [25]. These studies indicate that while cellulosic membranes may generally have lower permeabilities, their fouling resistance could lead to more sustainable reverse osmosis processes. Combining the low roughness of CAB membranes with the higher permeabilities of CTA and CAP would provide an alternative to TFCs in these applications.

Many operations have biological components early in the process, whether it is wastewater treatment or food production. To use reverse osmosis in these applications, expensive pretreatment processes must be used to protect the membrane from biofoulants reaching the membrane. A pervasive way to deal with this is by using disinfectants early in the process to kill off microorganisms so they can be removed early on. This leads directly to another problem that TFCs face; oxidative damage from disinfectants like chlorine and hypochlorite. Early studies of TFCs claimed that polyamide had solid resistance to chlorine, but these studies only demonstrated a

short-term resistance to chlorine [21]. As further studies were conducted, it became clear that TFCs cannot tolerate ppb levels of chlorine or hypochlorite without significant structural damage [26]. One study by Jung-Hyun Lee et al. in 2013 demonstrated that chlorine exposure makes the films more fragile, marked by an increase in elastic modulus and a decrease in fracture strength and onset of fracture strain [27]. This led to an increase in flux and a steep drop-off in selectivity. Cellulose acetate, on the other hand, can withstand a continuous exposure of 1 ppm of chlorine, making it the superior option in processes involving disinfection. The implications of this is massive, as even seawater desalination often has disinfection steps [2].

Given the ability of cellulose acetate-based membranes to overcome the limitations of polyamide TFC membranes surrounding biofouling and chlorine/hypochlorite resistance, additional investigation into cellulose-based membranes is warranted. There has been renewed interest in recent years in the development of a more competitive cellulosic thin film composite membrane by tuning the structure of the films. One study in Nature Communications in 2019 showed that a plasticizer treatment of a CTA thin film composite membrane changed the size of the crystallite sites in the film, allowing for a direct tuning of the transport properties of the membrane [28]. Having this level of control over the structural properties will allow for the creation of application-specific membranes. There is a need to understand the structural properties of the membranes and have the ability to tune these properties. To do this effectively, simple characterization techniques are required. Thin Film Elastic Modulus Characterization

One way to investigate the structure of a material is through its mechanical properties. Mechanical properties look at a material's response to external stresses applied. In a polymer, these responses reflect internal bonding, whether chemical or physical bonds, molecular density, and chain stiffness [27]. Mechanical properties reveal the structural properties of polymer films with

simple techniques. Due to the thickness of thin films, traditional elastic modulus characterization methods such as compression and tensile tests are not possible. One method to probe thin film mechanical properties is through surface wrinkling [29]. This technique, schematically shown in Figure 2.3, involves adhering a stiff thin film to a compliant, elastic substrate and applying a uniaxial tensile strain. A mismatch of stiffness between the film and substrate, causing mechanical instability as more strain is applied. At a critical strain, the film buckles and wrinkles with a well-defined wavelength begin to appear. Wrinkle wavelength can be determined through various techniques such as optical microscopy, laser diffraction, atomic force microscopy (AFM), or profilometry. Compared to other common techniques for determining thin film elastic modulus, such as AFM and nanoindentation, the wrinkling technique is relatively simply and more flexible [30] [31].

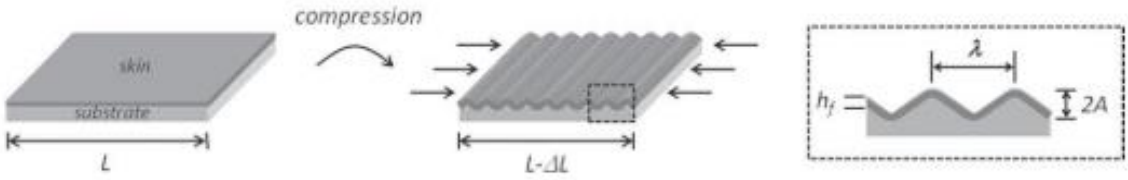


**Figure 2.3** – A depiction of surface wrinkling. Obtained from [32].

Buckling has been studied since the 18th century. When a beam is being compressed, there comes a critical strain where deflecting becomes easier than continuing to compress, leading to buckling. In the mid-20th century, the principles began to be applied to plates [32]. The stiffness of the films is an important component to the stability of the composite under uniaxial load, so the frequency at which the film buckles can be correlated to stiffness. The elastic modulus can be determined through the relationship:

$$\bar{E}_f = 3\bar{E}_s(\frac{\lambda}{2\pi h_f})^3 \quad (2.2.1)$$

$$\bar{E}_x = \frac{E_x}{(1-\nu^2)} \quad (2.2.2)$$

where $\bar{E}_f$ is the plane-strain elastic modulus, $E$ is the elastic modulus, $\nu$ is the Poisson's ratio, $h_f$ is the height of the film, and $\lambda$ is the wrinkle wavelength.

This technique is effective at measuring the elastic modulus of many polymer films, including polystyrene modified with plasticizers and UVO treatment, and polyelectrolytes [28] [33] [34]. One example showing the robustness of this model involved measuring the wrinkle wavelength of polystyrene films at different thicknesses yet showed that they had consistent elastic moduli (Figure 2.4) [29]. This is predicted by the model previously shown; if all else is equal, including elastic modulus, then the relationship between film thickness and wrinkle wavelength should be linear. Surface wrinkling has been used in many different studies to probe the structural properties of thin polymer films to investigate a variety of structural quirks. One example is from Christopher Stafford, where he demonstrated that in a polystyrene system, increasing plasticizer (dioctyl phthalate) content decreased the elastic modulus of the film, and these results were backed up with nanoindentation (Figure 2.5A) [29]. The same study looked at organosilicate thin films and showed an inverse relationship between elastic modulus and porosity, using nanoindentation as a secondary technique (Figure 2.5B) [29]. The models used in surface wrinkling are significantly simpler than nanoindentation and can be tested at a higher throughput, meaning a more straightforward process for probing the structural properties of thin films used in membranes.

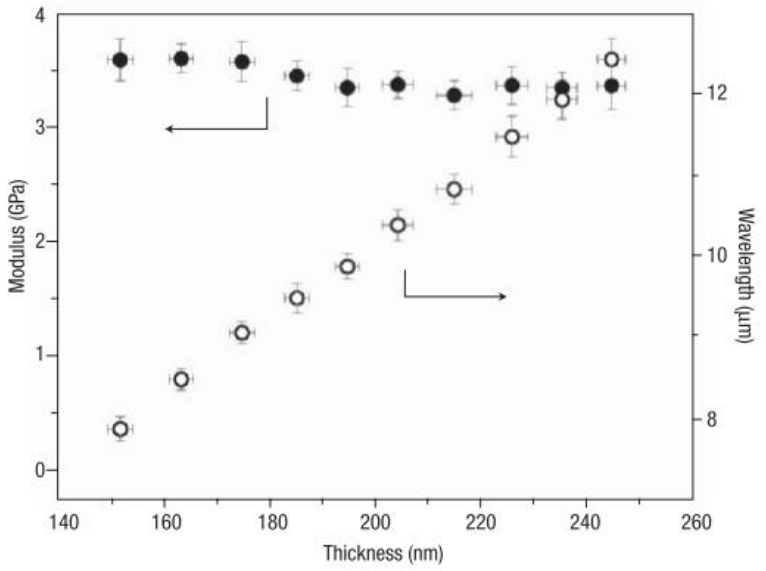


**Figure 2.4 -** The linear relationship between wrinkle wavelength and film thickness. Reproduced from [29].

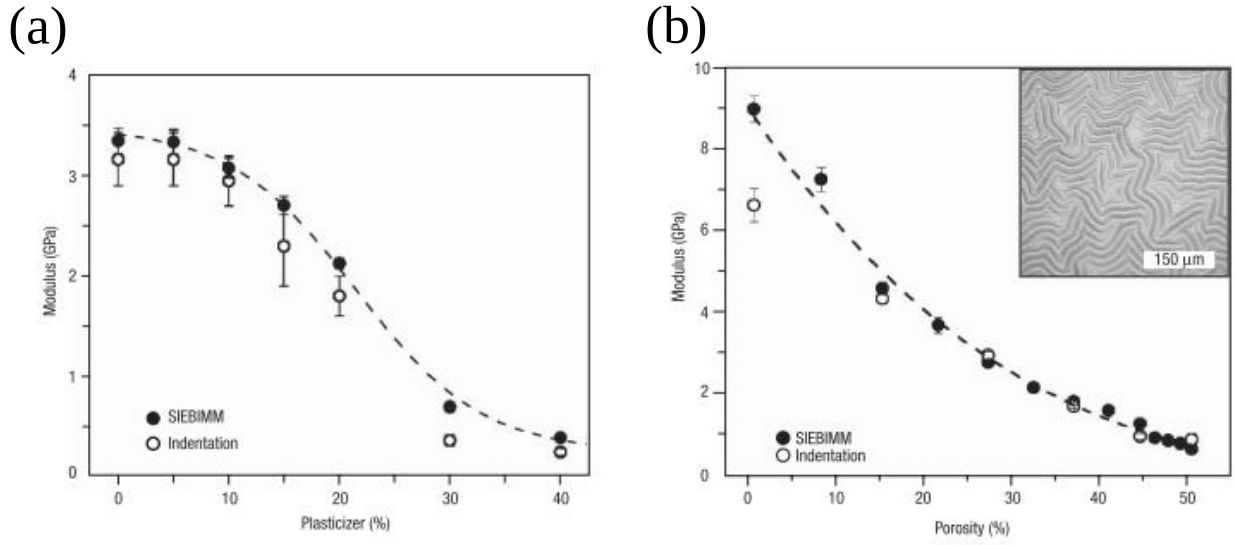


**Figure 2.5** – a) The relationship between elastic modulus of polystyrene thin films and plasticizer content. b) The relationship between the elastic modulus of organosilicate thin films and their porosity. Reproduced from [29].

One assumption in using Equation 1 is strong adhesion between the film and substrate. When surface adhesion is poor, an additional adhesion interlayer with well-characterized mechanical properties, such as polystyrene, can be incorporated into the film-substrate composite. This adhesion layer is placed between the PDMS substrate and the polymer film of interest. In this

scenario, a two-layer composite model may be used to analyze thin film mechanical properties. This model is summarized by the following equations [35]:

$$\bar{E}_f = \frac{\frac{\bar{E}_{eff}}{4} - \bar{E}_{PS}\left[\left(\phi_{PS} - \frac{\kappa}{2}\right)^3 + \left(\frac{\kappa}{2}\right)^3\right]}{\left(1 - \frac{\kappa}{2}\right)^3 - \left(\phi_{PS} - \frac{\kappa}{2}\right)^3} \tag{2.2.3}$$

$$\overline{E}_{Eff} = 3\bar{E}_s\left(\frac{\lambda}{2\pi d_t}\right)^3 \tag{2.2.4}$$

$$\kappa = \frac{1 + \phi_{PS}{}^2\left(\frac{\overline{E}_{PS}}{\overline{E}_f} - 1\right)}{1 + \phi_{PS}\left(\frac{\overline{E}_{PS}}{\overline{E}_f} - 1\right)} \tag{2.2.5}$$

where $d_t$ is the thickness of the two-film composite, $\bar{E}_{eff}$ is the effective film modulus of the composite is treated as a single film, $\phi_{PS}$ is the thickness ratio of polystyrene to the full composite, and $\kappa$ is a variable used to simplify the solution of the final equation. This model uses the elastic moduli of the polystyrene and PDMS substrate, the thicknesses of the polystyrene and film of interest, and the wavelength of the wrinkled films to find the elastic modulus of the film of interest. The system is solved iteratively, where an initial guess is made for the value of kappa, and the cellulose acetate modulus is adjusted to close the system. This model has been used in a previous study to determine the elastic modulus of polyelectrolyte film composites [35].

## 2.2. Thin Film Confinement

One phenomenon that has been studied extensively through the lens of surface wrinkling is thin film confinement [36] [37]. Thin polymer films tend to have a consistent elastic modulus regardless of the thickness. This is referred to as the bulk regime. As films get thinner, they remain consistent until there is a sudden drop in the elastic modulus. This phenomenon is termed "confinement," as the film is confined between its substrate and the air-film interface. Polymer

films of all sizes have this effect on their free surfaces, but if the film is thick enough, the properties of the rest of the film will dominate. When a film is thin enough, these surface effects begin to dominate the properties of the film. Early experiments into this phenomenon focused on its effects on the glass transition temperature. An early letter to the Physical Review by Forrest et al. in 1996 showed that for freestanding polystyrene films, the glass transition temperature depresses linearly with respect to film thickness at film thicknesses below 70 nm [38]. In a follow-up study, the group showed that the suppression of glass transition temperature was due to the interfacial effects of the polymer and the environment [39]. In 2005, a study by Ellison et al. reproduced earlier these confinement effects and additionally showed that molecular weight had little effect on glass transition temperature depression [40].

Studies into confinement have branched out into studying other phenomena. As mentioned earlier in this section, one of the phenomena affected by confinement is the elastic modulus; the rationale is that if confinement alters the organization of the polymer chains, it should reflect in mechanical properties. Early studies focused on polystyrene. Polystyrene has been considered the archetypal "model" system for studying confinement for decades [41] [42]. This is because it is a widely-available, commonly-used, well-characterized polymer that exhibits a dramatic change in its properties in confinement. In polystyrene, it has been shown that there is a depression in elastic modulus below 30-50 nanometers [43] [36] [44] [37] [33]. There is some discrepancy between nanoindentation and other characterization methods in polystyrene elastic modulus depression. The discrepancies between the thickness at which confinement begins indicates the importance of studying confinement from different angles through different phenomena to get a deeper understanding of the nanoscale structure of these films. Getting different length scales for different properties will allow for further correlation of these properties to transport properties.

The most common theory explaining confinement effects is that at the air-film interface, there is greater chain mobility [42]. This is supported by many different phenomena, such as the elastic modulus depression. Polymers with stiffer backbones, therefore less chain mobility inherently, have much less pronounced confinement effects [45]. Another study into cellulose thin films using x-ray scattering demonstrated that cellulose films have significantly higher free volume within 25 nanometers of the surface [13]. The mechanism of this phenomenon is important to investigate because it has implications on the use of thin polymer films in practice.

Confinement is of interest to membrane systems because it gives a lower limit for the thickness of a thin-film composite. A 2021 study demonstrated that molecular layer-by-layer (mLbL) thin polyamide membranes have a sharp drop in rejection and a massive rise in permeance at around 5-15 nanometers in thickness [46]. While the study did not directly attribute this to confinement, it works with the theory that polymers have significantly higher free volume at the surface, leading to a greater permeability. This sort of confinement was demonstrated earlier in a 2017 study into mLbL polyamide films showed that when exposed to high humidity levels, the thinner the film, the more it swelled. Understanding these phenomena allows for the prediction and tuning of transport properties.

### 2.3. Thin Film Swelling

As explained in the previous section, the swelling of polymer films can be connected to the transport properties of thin films. The swelling of a polymer is characterized by the volume change in a polymer exposed to different solvents at different concentrations. For a thin polymer film, swelling only needs to be considered in the direction normal to the film's surface. To quantify it, a swelling ratio is used [44]:

$$S_h = \frac{h_f}{h_0} \tag{2.4.1}$$

where $S_h$ is the swelling ratio, $h$ is the film thickness, and $h_0$ is the dry thickness of the film. To perform these measurements, the samples must be dried and have their thicknesses characterized to provide the baseline, and then the samples can be treated however necessary.

Swelling is driven by two competing forces: the enthalpic driving force of the mixing of the polymer and solvent, and the entropic and enthalpic resistance to the affine expansion of the polymer network. An early thermodynamic model for this system is described by Flory and Rehner [47]:

$$\Delta\mu_s = \frac{\partial \Delta G}{\partial n_s} = \frac{\partial \Delta G_{mix}}{\partial n_s} + \frac{\partial \Delta G_{el}}{\partial n_s} \tag{2.4.2}$$

If there is favorable interaction between the polymer and solvent, the solvent can permeate into the film through “unoccupied” free volume and begin to affect the intermolecular forces within sections of the polymer (Figure 2.6).

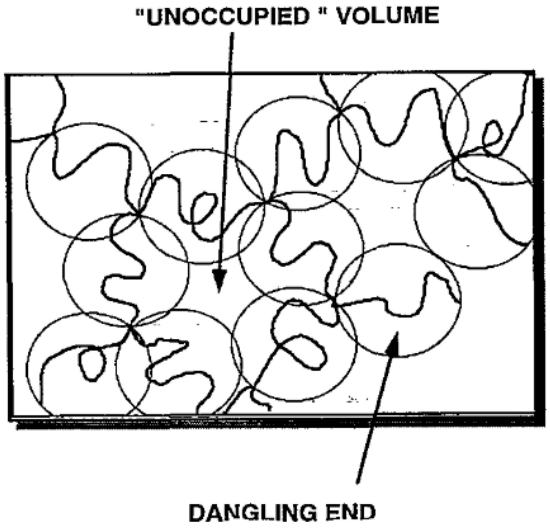


**Figure 2.6 -** A visual representation of a polymer network with unoccupied volume and "blobs" representing regions of strong intermolecular forces. Reproduced from [45].

Swelling measurements will reflect the structural properties of the polymer network, such as degree of crosslinking and free volume [44] [48] [49]. In one study, Edward Chan looked at layer-by-layer polyamide desalination membranes and demonstrated a difference in swelling activity based on the chemistry of the interfacial polymerization process [44]. In this case, the chemistry of polymer backbone of the membrane will impact simple measurements that have an impact on the transport properties of the membrane. Another example is cellulose acetate fiber mats, which have different regions of molecular mobility of water representing changes in the structure of the polymer as it is wetted (Figure 2.7) [50] [51]. The degree to which a polymer network swells gives information on the interaction between the polymer and solvent, and the resistance to swelling due to the breaking of intermolecular bonds within the polymer.

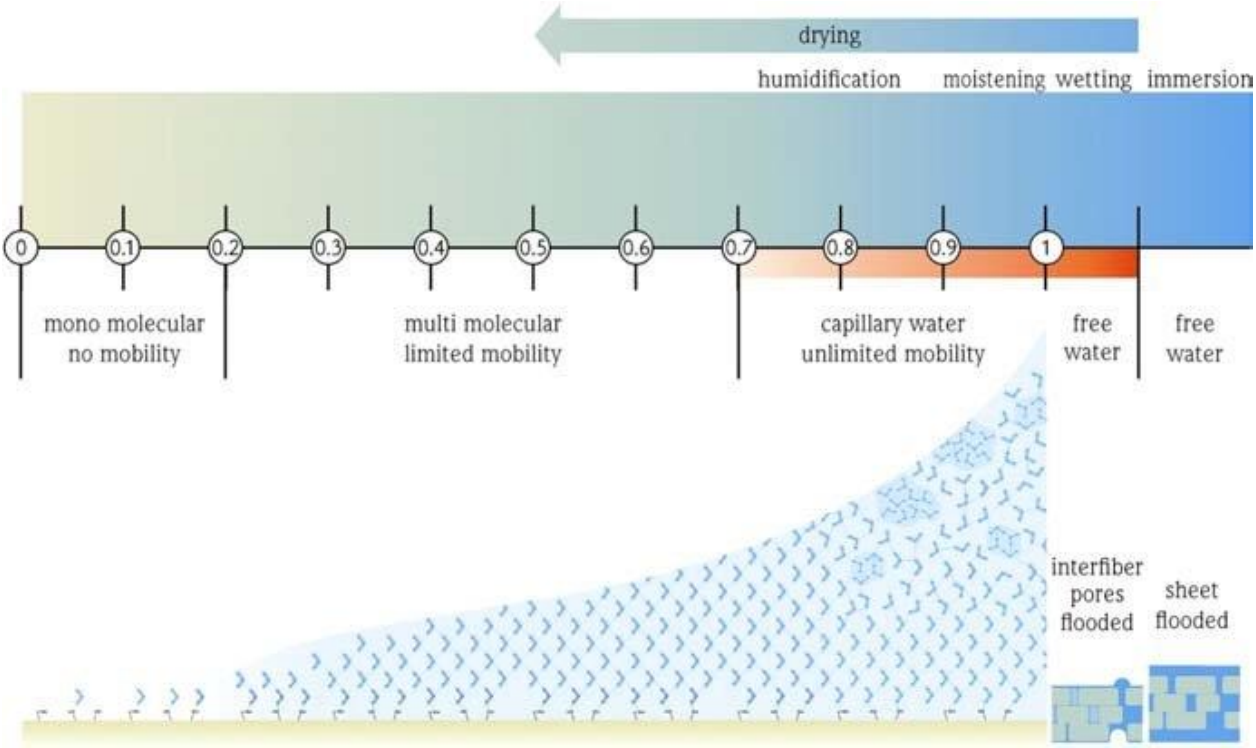


**Figure 2.7 -** The molecular mobility of water in cotton cellulose over varying levels of relative humidity. Reproduced from [29].

A simple way to analyze the swelling behavior of a material is using water as a solvent. In membrane systems, water will be the solvent, so understanding the structural changes that occurs due to water permeating through the film will be of interest for membrane materials. A study by Edward Chan et al. showed that by changing the chemistry of a crosslinked polyamide system, different swelling behavior can be observed and that it can be modeled to understand polymer film crosslinking density and its interaction potential with water [44]. This finding has implications for membrane systems, where the free volume of an active layer can be correlated to the permeability of water. Another study by Nolte et al. correlated changes in the relative humidity on the mechanical properties of thin films [35]. The group discovered that non-hygroscopic materials such as polystyrene have a much weaker change to its mechanical properties compared to more hygroscopic materials such as polyelectrolytes. This effect has implication for membrane materials, as their response to being submerged in water may change their structure, leading to a change in their permeability. Most membrane materials are hygroscopic to some respect so that water can permeate through them. Studying how a polymer film responds to the permeation of water is essential to understanding how they perform as membranes.

### 2.4. Polymer Film Additives and Treatment

Cellulose acetate is rarely used in its pristine state in membranes. Additives and treatments such as plasticizers and annealing are commonly used to change the properties of bulk polymers and polymer thin films. These treatments are designed to modify the structures of the polymers in a way that enhances their performances in their applications, so treatments for polymer designed for membranes should improve their performance properties.

The most obvious treatment of a polymer used in a membrane is soaking the membrane. Whether the membrane is soaked during manufacturing or in use, the membrane will be soaked in

water at some point in its use. One way that water affects a polymer film is through its structural rearrangement. Because of the interaction of water and the polymer molecules, the chain will rearrange, leading to a change in free volume. In this way, water acts as a type of polymer treatment known as a plasticizer.

Plasticizers have been used for almost a century to modify the properties, with early examples of nitrocellulose compounds and PVC being plasticized [52] [53]. These compounds make bulk polymers more flexible, and ultimately, easier to process at an industrial scale [54]. There are two main types of plasticizers, internal and external [54]. Internal plasticizers are often comonomers with a lower glass transition temperature, modifying the bulk properties of the system. External plasticizers are molecules added to the resin that use secondary forces to modify the structure of the polymer. The plasticizer can then be left in the final product or soaked out. There have been decades of research done into plasticizers, comparing the effects of many different organic esters and hydrocarbons on different polymer systems [54]. There are different theories as to how plasticizers achieve their intended effect. One is a "free-volume theory" that describes plasticizers as molecules that increase the free volume through its secondary forces [54]. This increase in free volume would lead to greater chain mobility in the polymer. Another theory is a "gel-theory" [54]. This theory proposes that for amorphous polymers with a gel structure, plasticizer interrupts the points of attachment within the gel. This would decrease the crystallinity of the amorphous polymer and decrease its resistance to deformation.

One oddity observed early in the research into plasticizer effects was a counterintuitive shift in properties at low plasticizer content. In a 1973 study, PVC treated with plasticizer exhibited higher tensile strength and embrittlement at low plasticizer concentrations [55]. This phenomenon has been termed "antiplasticization". Numerous studies have documented this effect on multiple

different polymer-plasticizer systems. Research into this phenomenon has been scattered, and different hypotheses have been proposed to explain it. One is that the plasticizer's interactions at low concentrations decrease the free volume in the system. This hypothesis was proposed in a 1988 study that observed that at low concentrations of plasticizer, the specific volumes of the polymer and plasticizer are not additive, indicating a change in the packing of the structure [56]. Another theory is that plasticizers allow the polymer chain to "relax" by helping it overcome activation energy barriers and relax to a more thermodynamically stable state [57]. This has been demonstrated through dynamic mechanical analysis of cellulose acetate and polycarbonate.

Plasticizers are very frequently used in membrane systems to modify their transport properties. One study by Jian-Hwa Guo demonstrated that changing the amount of triacetin, a plasticizer for cellulose acetate, generally increased the permeability of the film except at low concentrations, indicating that antiplasticization had an impact on transport properties [58].

## 3. Materials and Methods

### 3.1. Description of the Major Equipment Used

#### 3.1.1. Texture Analyzer

A Shimadzu Trapezium X texture analyzer, shown in Figure 3.1, was used for compression testing and indentation experiments. The device consists of a load cell that can hold different probes and a stage for a sample. Two probes were used in this study: one cylinder with a flat face for compression testing, and a probe with a metal sphere tip for indentation testing. The load cell is moved at a constant rate while measuring the force applied to it. The maximum load for the device is 200 N.


**Figure 3.1** - The Shimadzu Trapezium X texture analyzer pictured with the attachment used for compression testing.

In reflectometry, the reflectivity of a thin film on a substrate depends on the wavelength of the incident wave [59]. A plane wave hits the sample and is partially reflected and transmitted at the interfaces between the air, film, and substrate repeatedly, and the resulting reflected waves are superimposed into one reflected wave. The thickness of the thin film will modify the amplitude of the resulting wave. Repeating this over a range of wavelengths will result in a relationship between amplitude and wavelength, which Frensel's laws can model.

Thin film thickness was characterized via reflectometry using a Filmetrics F20 Thin-Film analyzer (Figure 3.2). The device shines a light on a sample placed on the stage, and the resulting reflectance spectrum is analyzed in the Filmetrics software. Light is supplied by a tungsten-halogen bulb and is delivered to the device with a fiber optic cable. The reflected light is then measured at 1024 different wavelengths using a linear photodiode array that integrates the current generated by the 1024 pixels.

**Figure 3.2 -** F20 Thin Film Analyzer setup for reflectometry experiments.

3.1.2. Ellipsometer

Ellipsometry analyzes how a sample modifies the polarization state of an incident electromagnetic wave [59]. The change is quantified by two angles: Ψ and Δ, represented in the below equation.

$$\rho = \tan\Psi e^{i\Delta} \qquad (3.1.3.1)$$

Ψ is an angle corresponding to the ratio of the reflection coefficients in the parallel and orthogonal directions, while Δ corresponds to the phase difference between the components. These quantities change based on the wavelength of light and can be modeled as a spectrum based on the properties of the system. For thin polymer films, a common model is the Cauchy dispersion equation [60]. This model represents the index of refractivity as a 3-term polynomial. To model the surface roughness at the surface of the film, a Bruggeman Effective Medium Approximation layer is used [60]. This model is a weighted average of the dielectric properties of air and the substrate. Fitting this model to the Ψ and Δ spectra allow for the determination of the film thickness. The

primary advantage of ellipsometry is its ability to filter out effects from diffuse scattering. Because what is measured is the change in the polarization, even if some of the beam is lost due to being scattered by dust particles or surface roughness, the change in the polarization state can be characterized. This makes ellipsometry an accurate and reproducible method for film thickness determination.

**Figure 3.3 -** The ellipsometer used in from the M.I.N.D.s facility. It has a stage for the sample and an adjustable source and receiver that can be manually adjusted with the stage.

### 3.1.3. Strain Stage

The strain stage used for wrinkling experiments is shown in Figure 3.4. The design of this device was similar to a design previously developed by Stafford, et. al. [61]. Samples were placed in the stage to immobilize the substrate-film composite, which enabled performing film transfers without the risk of pre-straining/fracturing samples. The strain stage was connected to a stepper motor to control the amount of strain applied to the film-substrate composite.

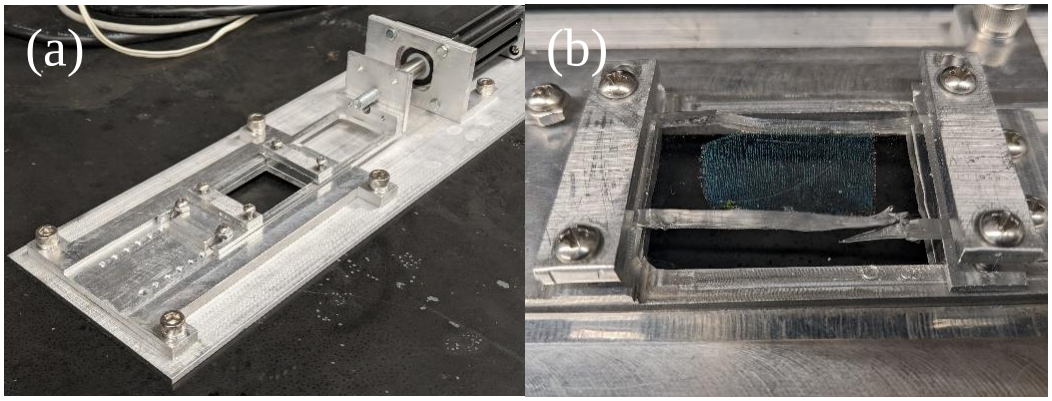


**Figure 3.4 -** a) The strain-stage fabricated at Rose-Hulman. b) A sample loaded onto the stage. The transparent portion is the PDMS substrate and the translucent blue-green portion is film.

### 3.1.4. Humidity Box

The humidity box used for swelling experiments is shown in Figure 3.5. The device was acquired and configured by Dr. Adam Nolte of the Rose-Hulman Institute of Technology Chemical Engineering Department and consisted of a 61cm x 45 cm x 38 cm plexiglass box with a door to seal the contents from the external environment. Humidity was controlled with an ETS Dual Control Model 5200 control system. To increase the humidity, the box was hooked up to a humidifier controlled by the controller. To decrease the humidity, the box was hooked up to house air controlled by a solenoid valve that opens and closes based on signals from the controller.

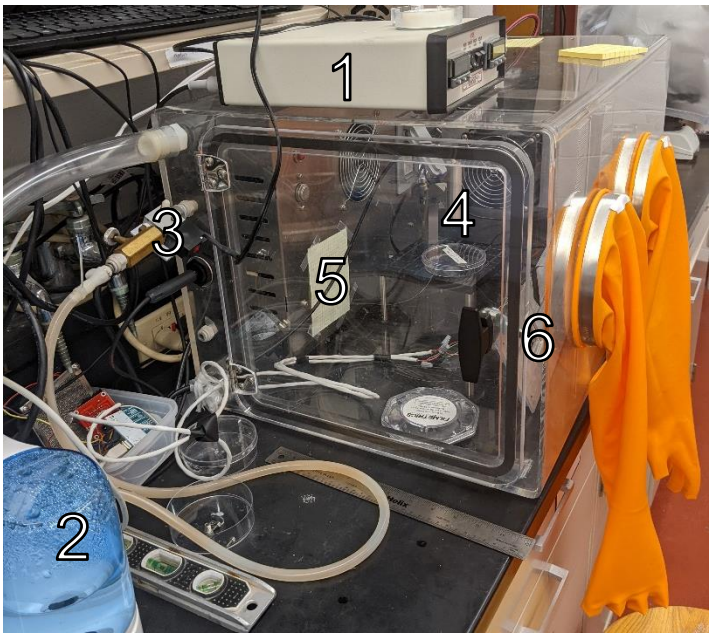


**Figure 3.5 -** The humidity box used for climate-controlled experiments. 1) The control module 2) The humidifier 3) The solenoid valve 4) The reflectometer 5) The diffraction screen 6) The strain stage.

## 3.2. Experimental Protocols

### 3.2.1. Thin Film Fabrication

Polymer thin films were prepared via spin coating. In this process, a casting solution is poured onto a substrate. The substrate is spun at a given speed for a set amount of time. During this process, the solution is spun off the substrate, and the remaining solvent evaporates, leaving behind a thin polymer film. Film thickness can be controlled by the adjusting spin speed and concentration of the polymer casting solution.

Silicon wafers, cut into 2 cm x 2.5 cm rectangles, were used as substrates for the spin coating process. Wafers were cleaned first by a series of three 15-minute sonication steps in acetone, methanol, and ultrapure DI water, respectively. The substrates were then dried with house air and treated using Novascan PSD Series Digital UV Ozone System for 30 minutes, immediately before spin coating.

Cellulose acetate butyrate (CAB) used for thin film fabrication was purchased from Sigma Aldrich. It had number average molecular weight of ~30,000 g/mol and contained 12-15 wt% acetyl groups and 36-40 wt% butyryl groups. Casting solutions contained 0.5-2.5 wt% CAB dissolved in ethyl acetate. For CAB films containing triacetin, triacetin from Sigma Aldrich (CAS: 102-76-1) was added directly to the CAB casting dope at appropriate quantities to achieve polymer films containing 5-40% triacetin by weight. From here on out, any reference to percent triacetin is a weight percent in the final spun film. To remove triacetin after film fabrication, films were soaked in DI water for 30 minutes.

To create bilayer films for mechanical property testing, a release layer was cast onto a silicon wafer, with subsequent layers (PS adhesion layer or CAB layer) cast on top of the release layer. The release layer contained 1 wt% PSS in water, and the adhesion layer contained 2 wt% PS in toluene. All CAB, PSS, PS thin films were prepared using spin speeds ranging from 800 RPM to 3000 RPM and spun for 30 seconds. Other, standalone PS films for mechanical property characterization were prepared using conditions similar to those described above.

### 3.2.2. Thin Film Thickness Characterization

Film thickness was characterized through both reflectometry and ellipsometry. Reflectometry was carried out with a F20 Thin-Film Analyzer and validated with another reflectometer of the same model in the M.I.N.D.s. facility at Rose-Hulman Institute of Technology. In this study, reflectometry models were constructed using built-in models in the Filmetrics software or models for materials with similar optical properties (n=1.46869). For more complex samples with multiple layers, ellipsometry was used to characterize film thickness. For each measurement, 3-angles were used (65°,70°,75°), and each layer was modeled with a Cauchy dispersion model with optical properties obtained from Filmetrics and fitted to the sample.

### 3.2.3. Substrate Fabrication and Elastic Modulus Characterization

In this work, PDMS (Sylgard 184, Dow Corning) was prepared by mixing base and cross-linking agent at a 10:1 w/w ratio. The mixture was poured into various petri dishes to have thin and thick PDMS samples. The samples were then degassed and baked at 75°C and 10 in$H_2O$ of vacuum before being removed. The thin PDMS samples were cut into 2 cm x 5 cm strips and the thick samples were cut into 32 cm diameter disks.

One way to determine the elastic modulus of the substrate is through the use of contact mechanics, specifically, indentation. Indenting a material with a spherical probe while tracking its stroke and force will result in a curve like in Figure 3.6. These curves can be modeled with different methods, the most reliable of which is reported in the Journal of Colloid and Interface Science [31]. This method uses the work of adhesion found at the absolute minimum of the unloading curve and the point at which the adhesive and compressive forces cancel each other out and produces a "reduced modulus":

$$E_r = \frac{-3P_{adh}}{\sqrt{R}}\left[\frac{3(\delta_0 - \delta_{adh})}{1 + 4^{-2/3}}\right]^{-3/2} \tag{3.3.1}$$

$$\frac{1}{E_r} = \frac{1 - \nu_i^2}{E_i} + \frac{1 - \nu_s^2}{E_s} \tag{3.3.2}$$

where $E_r$, $E_i$, $E_s$ are the reduced modulus, modulus of the indenter, and modulus of the sample, respectively, $P_{adh}$ is the force of adhesion $\delta_0$ is the stroke at which the net force on the probe is zero, $\delta_{adh}$ is the stroke at which $P_{adh}$ is reached, and $\nu_i$ and $\nu_s$ are the Poisson ratios of the indenter and sample, respectively. In indentation experiments, the absolute minimum of force-stroke curves was used as the force and stroke of adhesion.

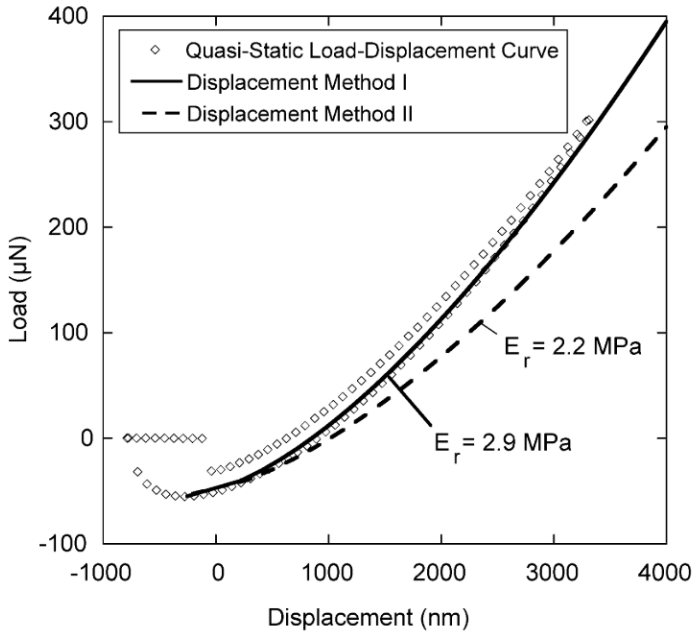


**Figure 3.6 -** Typical JKR loading and unloading curve with two methods for fitting it. Obtained from [31].

Another way to determine the elastic modulus of the substrate is through compression testing. Compression tests using the Shimadzu EZ-SX 200N texture analyzer were performed on the disk samples to find the elastic modulus of the substrate ($E_s$). The stage and probe were lubricated with silicone grease to decrease the effect of surface adhesion of the samples. The elastic modulus was then taken as the linear region between 10%-20% strain; where full contact was established, and surface effects were not significant.

### 3.2.4. Thin Film Elastic Modulus Characterization

Thin film elastic modulus values were determined through surface wrinkling, according to the protocol described by Stafford et al. [29]. Films containing a polystyrene-sulfonate (PSS) release layer were placed face down onto a PDMS substrate affixed to the strain stage. The strain stage/film setup was then immersed in water for at least 30 minutes to dissolve the PSS layer, separating the polymer film from the silicon wafer and leaving it adhered to the PDMS. A uniaxial strain was then applied to the PDMS-film stack, resulting in surface wrinkles (Figure 3.7a).

Multiple photos were taken with an optical microscope and analyzed with a fast-Fourier transform (Figure 3.7b). The FFT analysis will allow for measuring the average wavelength in the image.

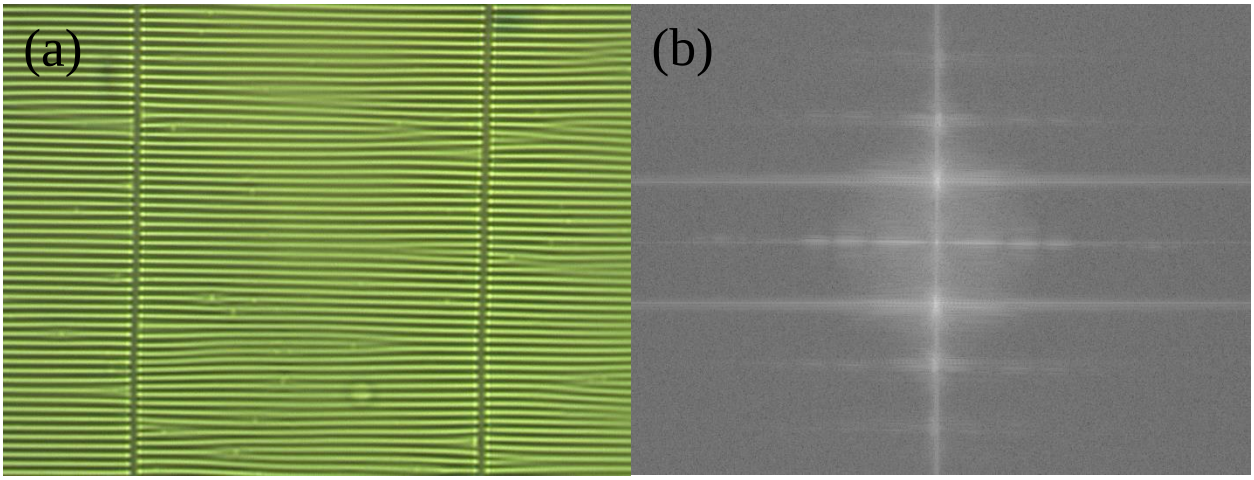


**Figure 3.7 -** a) A microscope image of a film wrinkled and cracked. b) An FFT image of Figure 3.7a.

Another method for characterizing wrinkle wavelength is laser diffraction, which is based on Laue-Bragg interference. The governing equation used for these measurements is as follows:

$$n\lambda = 2d \sin\theta \tag{3.3.1.1}$$

where $n$ is the diffraction order, $\lambda$ is the wavelength of the laser pointer, $2d$ represents the length between the laser point and the first diffraction point, and $\theta$ is the angle between these two points. Wrinkle wavelength was determined using this approach for all experiments performed in a controlled humidity environment, since the optical microscope could not be moved into the humidity box described in §3.1.5. In the experiments that required humidity control, the strain stage with the sample mounted was placed vertically in the humidity box. A laser pointer of varying wavelengths ($\lambda$ = 532 nm and 654 nm) was shone horizontally through the sample and onto grid paper for measurement. Films were equilibrated at 5% relative humidity for an hour, and the films were swelled by increasing humidity. When humidity was increased, films were equilibrated for 30 minutes before being strained and had their elastic modulus values measured.

#### 3.2.5. Swelling Experiments

Humidity measurements were carried out in the humidity box described in §3.1.5. Films were equilibrated for at least 30 minutes at 5% relative humidity before experiments. Film thickness was measured with the reflectometer at this humidity to provide a dry thickness of the film using the average of 3 spots towards the film's center. Films were then exposed to increasing humidity at levels of 20%, 40%, 60%, and 80% relative humidity, equilibrating for 30 minutes at each humidity step.

## 4. Results and Discussion

### 4.1. Cellulose Acetate Butyrate Swelling Behavior

In this work, the goal was to modify the structure of cellulose acetate butyrate (CAB) thin films and observe these changes through simple measurements. The simplest method this study used to analyze the effects of different treatments on CAB films was swelling measurements. With accurate measurements of film thickness and control over factors such as film thickness, humidity, and film treatment, different structural phenomena such as confinement, plasticization, and antiplasticization can be observed solely from changes in film thickness.

#### 4.1.1. Pristine Cellulose Acetate Butyrate Swelling

The objective of this work was to have the ability to tune the structure of the CAB films. An important aspect of this is to have control of the thickness of the CAB films so that thickness related effects can be studied. CAB films of varying thicknesses, spanning both the confined and bulk regimes, were prepared via spin coating. Films were spun using 0.5%, 1%, 1.5%, 2%, and 2.5% CAB solutions in ethyl acetate at 3000 RPM for 30 seconds to fabricate films of 15 to 150 nm in thickness. This was confirmed by measurements and model fits from two different reflectometers and one ellipsometer were compared (Figure 4.1). Thickness values determined for

each instrument as a function of CAB film thickness were comparable, as shown in Figure 4.1. Given the agreement between the three instruments, the CHE reflectometer was used for most future experiments and was incorporated into the humidity box set-up.

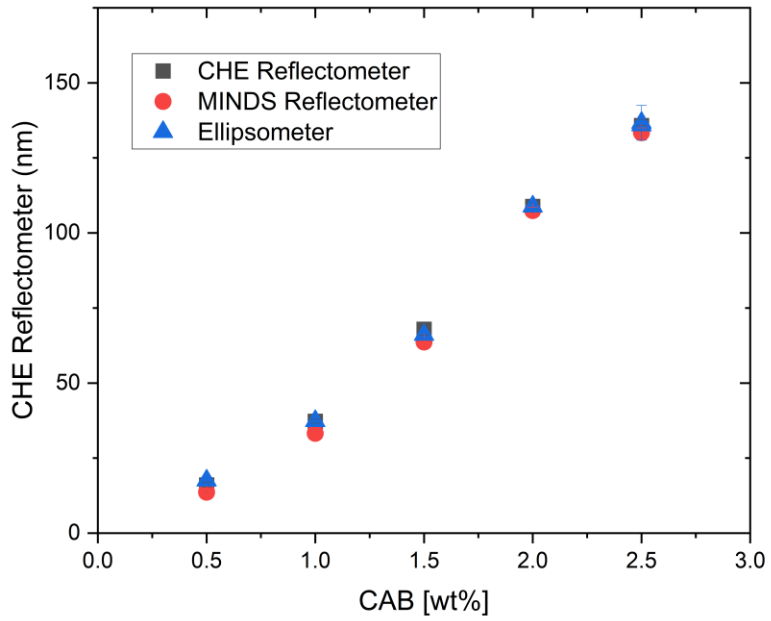


**Figure 4.1 -** Film thicknesses as a function of CAB wt% of films spun at 3000 RPM for 30 seconds.

After establishing control over the spun thickness of the CAB thin films, swelling properties were investigated. Because these films were so thin, it needed to be established that swelling activity could even be detected through reflectometry. Polystyrene films exhibited no change in thickness with humidity which is to be expected from a highly hydrophobic polymer. CAB, on the other hand, is moderately hydrophilic. Preliminary swelling experiments for CAB were carried out on four CAB films ranging from 100 to 250 nanometers in thickness. All four films were in the bulk regime and soaked in DI water for 30 minutes before being equilibrated at 5%, 20%, 40%, 60%, 80% humidity for 30 minutes. Figure 4.2 shows that while the change in film thickness of the films is minor, being less than 5 nanometers, but when comparing their

swelling ratios, there is remarkable agreement (Figure 4.2). These films have significantly higher swelling activities than non-hygroscopic materials such as polystyrene. Still, they are less active than common membrane materials like different polyamide compounds because CAB is more hydrophobic than polyamide due to its large butyryl groups. [44] [48]

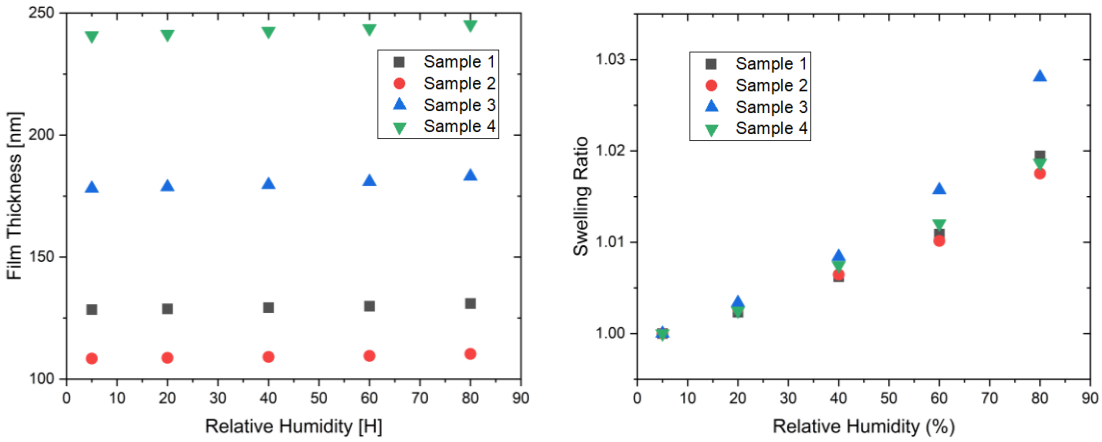


**Figure 4.2 -** Swelling behavior of water-soaked CAB films. a) Thickness change as a function of increasing humidity. b) Swelling ratio as a function of increasing humidity.

The swelling behavior of confined films with thicknesses less than 20 nm was compared to that of films with thicknesses in the bulk regime, each of a thickness greater than 100 nm. As shown in Figure 4.3, the confined films have significantly higher swelling ratios than bulk films, especially above 60% relative humidity. Figure 4.4 shows the effect of film thickness on the maximum swelling ratio. This plot shows an obvious bulk regime with a swelling ratio of around 1.02-1.03 for all films above 70 nm in thickness. At around 50 nm, there is a small increase in the maximum swelling ratio, but the effect becomes much more significant as the films get thinner, with a swelling ratio of 1.15 observed for films 26.4 nm thick. Unlike in the bulk regime, the swelling ratio of confined films is thickness dependent, beginning at a thickness somewhere between 45 and 70 nm. A previous study on the swelling of cellulose triacetate films reported a similar phenomenon, showing that crystallinity significantly decreased in this range [62].

Crystalline sites resist affine expansion due to the bonds in the crystal structure. Therefore, the decrease in crystallinity decreases the resistance to expansion, increasing its swelling activity.

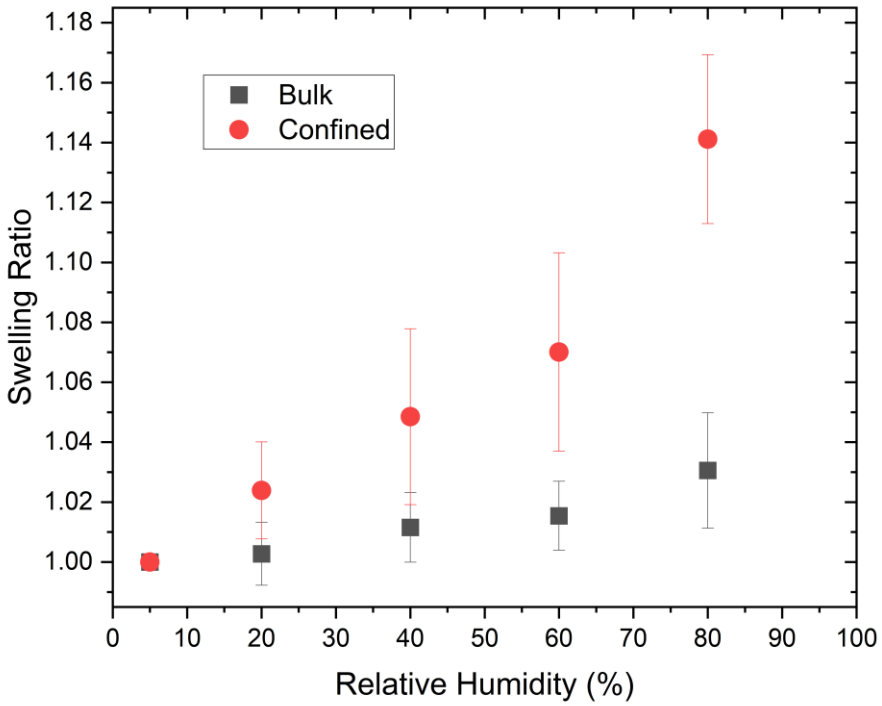


**Figure 4.3 -** The effects of confinement on the swelling. Confined films ($N = 4$) were each ~20 nm thick and bulk films represent four random samples all greater than 100 nm thick All films were soaked in water for 30 minutes and then equilibrated for 30 minutes prior to measurement. Error bars represent the standard deviation of the sample.

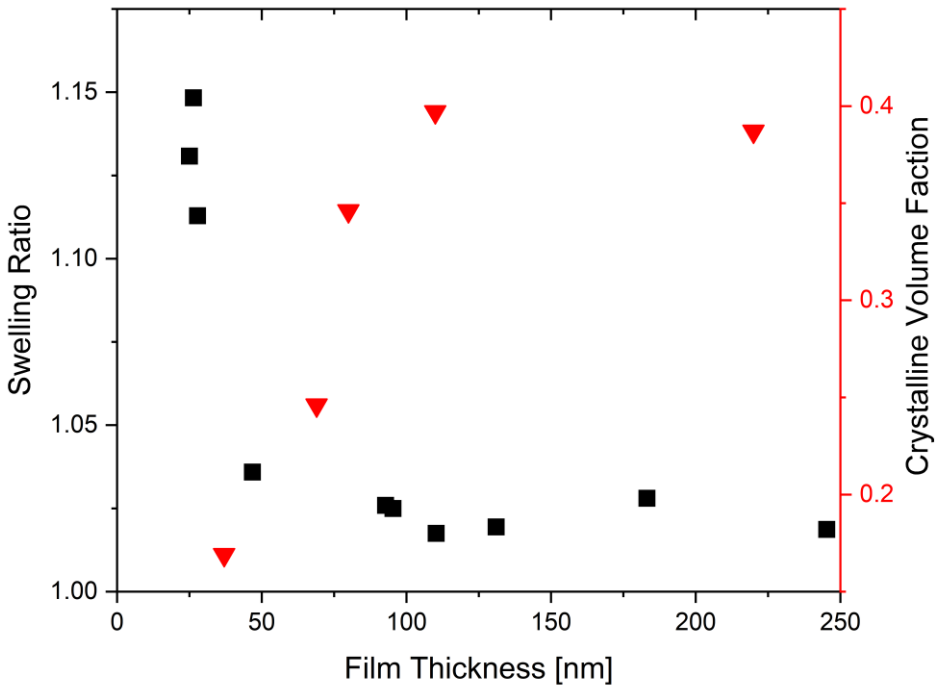


**Figure 4.4 -** The maximum swelling ratio plotted over a range of dry thicknesses. The change in swelling behavior is correlated to crystallinity changes. The maximum swelling ratio is defined as the swelling ratio at 80% relative humidity, and the film thickness is defined as the film thickness at 5% relative humidity. Crystallinity data obtained from [62].

### 4.1.2. Swelling of Treated Films

The objective of this work is not only to observe the structural effects of these films, but to modify their structural properties through treatment. Bulk regime cellulose acetate had their swelling behavior compared pre-soak and post soak (Figure 4.5). Soaked films had a reduction in swelling ratio of about 0.11 compared to unsoaked films. Previous studies have suggested that water acts as a plasticizer in these systems, causing structural rearrangement. The post-soak films have a higher resistance to swelling, indicating that the soaking process allowed the film to rearrange into a more thermodynamically favorable state with water acting as a plasticizer [54]. Understanding these treatments in thin polymer films has implications for membrane systems because membranes will be submerged in water, whether as a treatment or in operation. One

attempt at fabricating a CA TFC showed that the transport properties of the membrane significantly changed based on the time it was soaked in a water bath [63]. This is a relaxation behavior similar to what is reported here; water allows the polymer chain to relax into a more thermodynamic state.

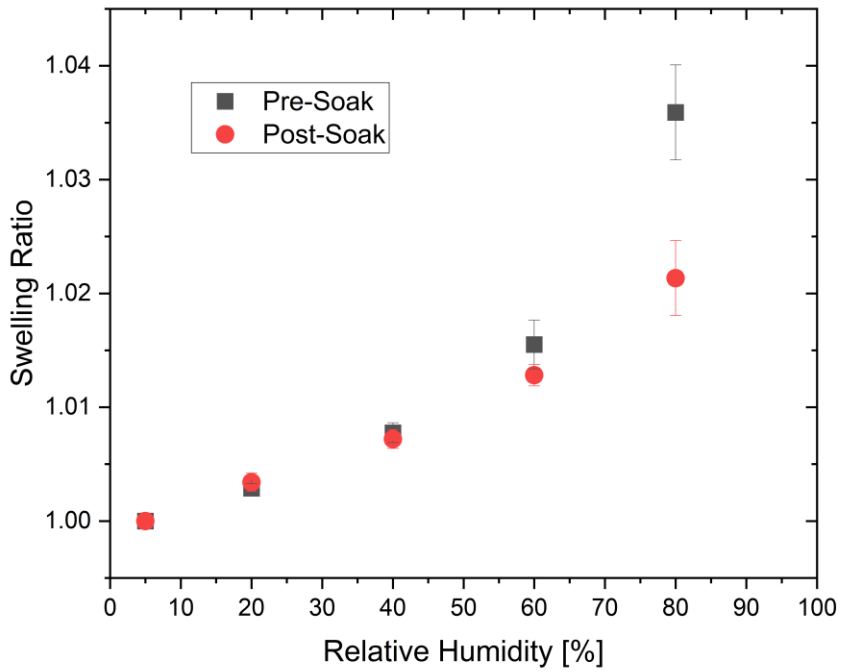


**Figure 4.5 -** Comparison of the swelling ratio before and after soaking the films. Each point represents at 4 trials at random thicknesses in the bulk regime with error bars representing the standard deviation of the group

While water's effect on a polymer film is of interest when studying membranes, it is an unavoidable and unchangeable fact of membranes. If tuning is the goal, there needs to be a change in the casting dope or fabrication process. Triacetin treatment is a more traditional plasticizer used to modify the structure of the CAB films. It has been used as a plasticizer to soften CAB for almost a century [64]. The simplest way to observe the effect of triacetin modification is through fabricating these films and observing changes in the film when the triacetin is soaked out. Films with varying levels of triacetin in the casting dope were spun and had their thicknesses measured before and after a 30-minute DI water soaking treatment at room humidity. In this treatment, the triacetin in

the casting dope will diffuse out of the film because of its solubility in water. In the bulk regime, pristine samples tend to have minimal changes in thickness during the soaking process, but there is a steady decline in the post-soak to pre-soak ratio with increasing triacetin weight percent, decreasing almost 10% in thickness at 40% triacetin (Figure 4.6). The general trend shows that with increasing triacetin content, there is a greater amount of "relaxation" within the films. Interaction between the plasticizer and the polymer chain combined with the soaking process. It has been demonstrated in the literature that plasticizer increases the free volume within the polymer [56]. When the triacetin is soaked out, the polymer is can relax to a more thermodynamically stable state [57].

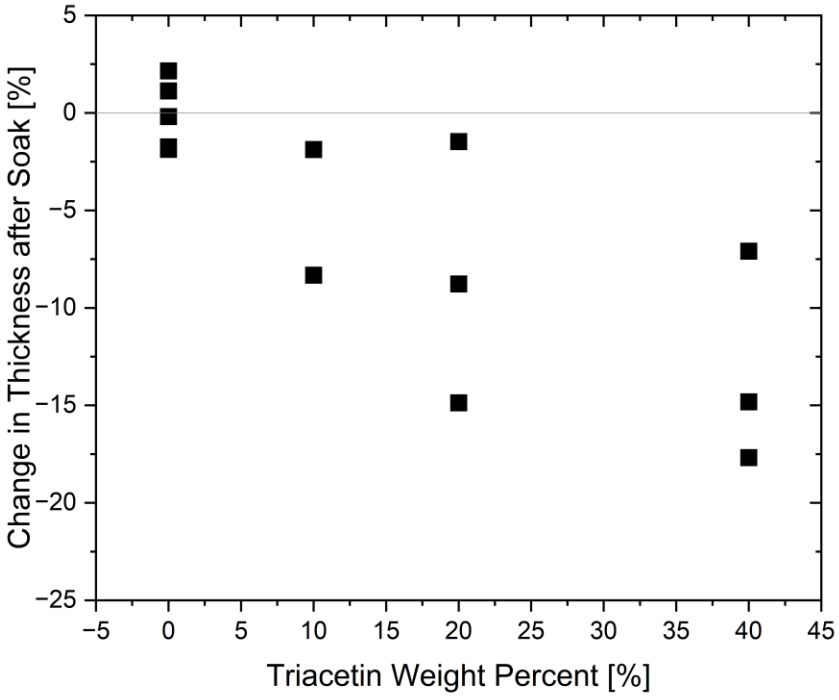


**Figure 4.6 -** The decrease in thickness at room humidity at varying triacetin levels in the bulk regime. Error bars represent the measurement error. The red line represents 0%, or no change in thickness.

Films with varying levels of triacetin treatment had their swelling behavior analyzed. With samples treated with triacetin in the casting dope, but no soaking process to remove triacetin (acting as an internal plasticizer), there is a wide range of swelling behavior, but on average, deswelling behavior when exposed to humid conditions (Figure 4.7a). Films with the triacetin soaked out of them exhibited more similar swelling behavior to pristine samples (Figure 4.7b). The difference between these two indicates that the resistance to swelling seen in the unsoaked samples is due to the triacetin within the film. Most internal plasticizers tend to be very bulky molecules, such as di(2-ethylhexyl) phthalate, di(isodecyl) phthalate, and di(2-ethylhexyl) adipate [65]. They are designed to bond with the polymer backbone and "space out" the chains so that they can move more freely. Triacetin is a significantly smaller molecule than these other internal plasticizers, so it cannot fulfill that function. Instead, it forms secondary bonds with the polymer chain, restricting movement [64].

Samples treated with the plasticizer and having the plasticizer removed showed swelling behavior closer to pristine CAB films but contained some peculiarities in the kinetics of swelling. To investigate the swelling of these samples, longer swelling experiments were performed where after being dried, the films were exposed to humid conditions and allowed to swell (Figure 4.8). The general behavior is that in the first 30 minutes, there is a relatively fast growth in thickness, but the swelling slows for the next 30 minutes and going forwards. This indicates a kinetic aspect to the swelling of the films, with fast swelling initially when exposed to the chemical potential gradient, and a slower growth over longer periods. The initial growth comes from the permeation of water into the polymer matrix spacing out the side chains while the slow growth is from the slower rearrangement of the chains while exposed to water. In the fast growth period, films at 10%

and 20% triacetin swelled notably less than the pristine films while 40% triacetin swelled more. Samples at 0% and 40% stopped swelling at this point, the 10% and 20% continued to swell.

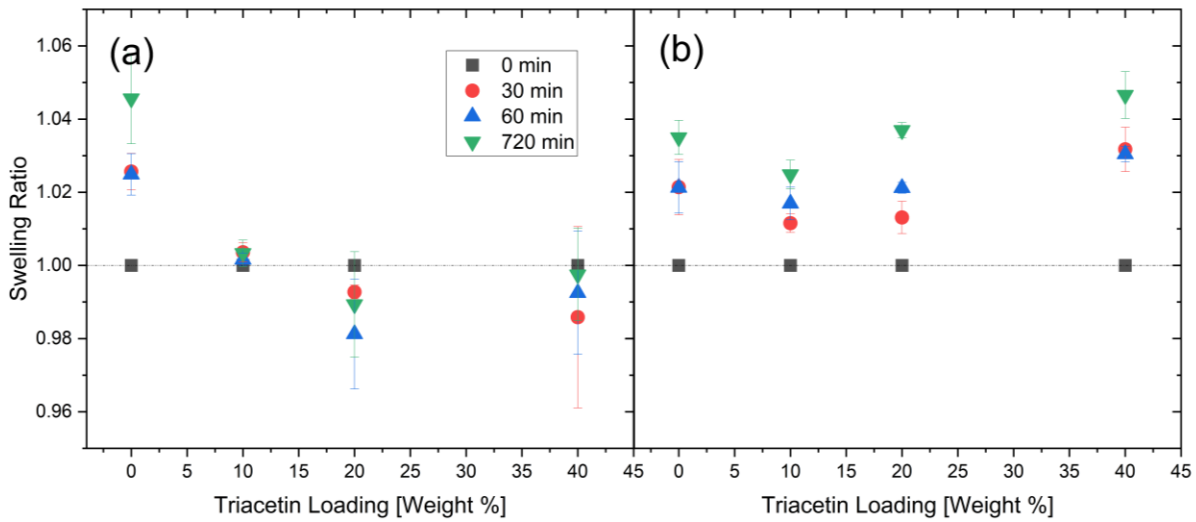


**Figure 4.7 -** a) Swelling ratios of triacetin-treated films without a soaking process at varying triacetin levels and time swelling. b) Swelling ratios of triacetin treated films with a soaking process at varying triacetin levels and time swelling. The dotted line represents a swelling ratio of 1, or no change in thickness. Error bars represent standard deviation of the group.

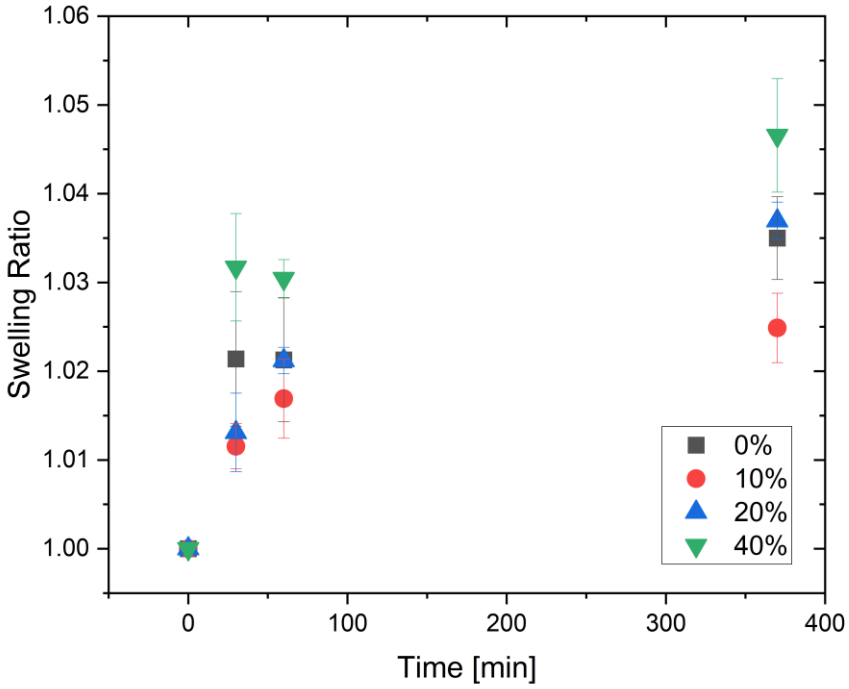


**Figure 4.8 -** The long-term swelling behavior of films treated with triacetin. Error bars represent standard deviation of the group.

After 720 minutes of swelling, the swelling ratio increased from 10% to 40%, and decreased from 0 % to 10%. The increase in swelling ratio between 10% and 40 % triacetin contents is attributed to a decrease in crystallinity as plasticizer content is increased [66]. With decreasing crystallinity, the polymer becomes more permissive to affine expansion. Crystalline sites resist expansion to maintain their crystalline structure, while the amorphous sections can adjust. Triacetin's disruptions of these sites leads the film to be more permissive of swelling. The exception to the general trend of increasing swelling activity with increasing triacetin content is at 10 wt% triacetin, which has a decreased swelling activity. This is interesting because this exception to the general plasticization trend was seen in data from Guo et al. [58]. In this study, Guo fabricated cellulose acetate thin films and performed permeability experiments, obtaining the results in Figure 4.9.

The question of interest is what causes this antiplasticization effect. Several studies done on other polymer systems demonstrated that changes in crystallinity cannot explain antiplasticization. This is affirmed in X-ray scattering data of triacetin-treated cellulose acetate films. These films do not show a significant difference in crystallinity between pristine CA films and 10% triacetin-treated films [66]. What is more likely occurring is that the small amount of triacetin-treated increases the free volume of the polymer matrix without disrupting the crystalline sites of the film. When the triacetin is soaked out, the polymer film can relax into a more thermodynamically stable state without changing its crystallinity. This demonstration of antiplasticization through swelling data shows that we can connect fundamental polymer phenomena to transport properties, and these phenomena can be investigated without the creation of membranes.

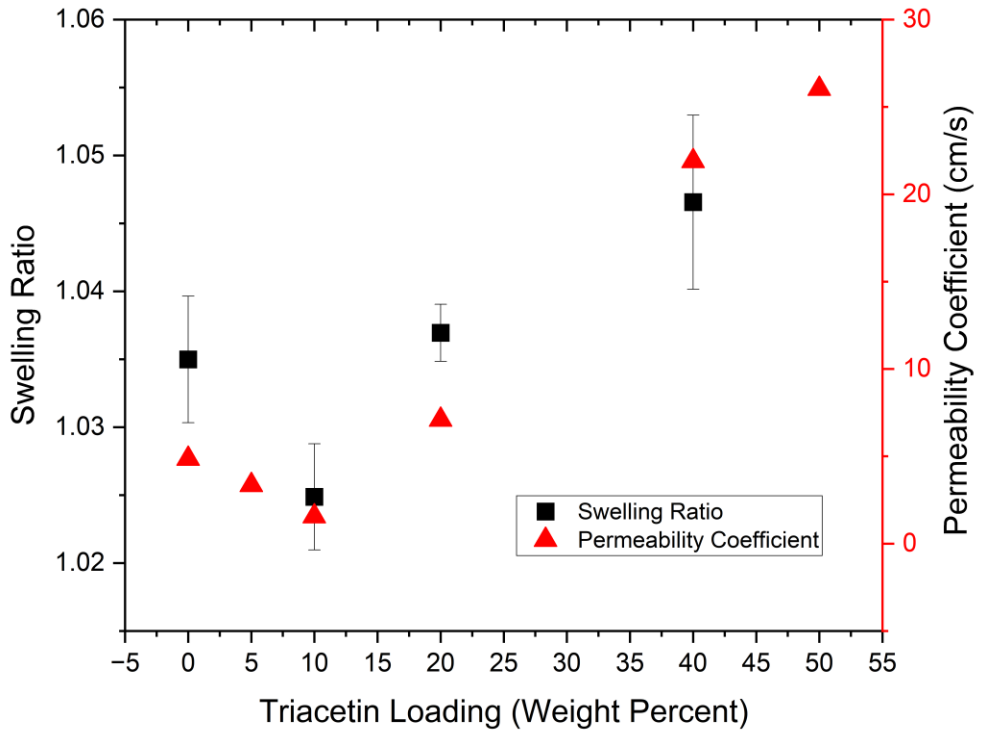


**Figure 4.9 -** Swelling ratio of triacetin treated and soaked thin films at 80 RH% (this study) compared to permeability data reproduced from Guo, et. al. [58].

## 4.2. Cellulose Acetate Butyrate Mechanical Properties

To further explore confinement and antiplasticization effects in CAB thin films, thin film elastic modulus was characterized using the surface wrinkling technique. Previous studies have demonstrated that the mechanical properties of thin films can be used to probe different effects important to membrane separations, such as chlorine oxidation [27]

### 4.2.1. Wrinkling of a Model Film

Obtaining accurate thin film modulus values via surface wrinkling requires precise characterization of several parameters, including substrate modulus, thin film thickness, and wrinkling wavelength. Before characterizing CAB films, the modulus elasticity of polystyrene was characterized via surface wrinkling. Polystyrene thin films have been extensively characterized

using this technique and therefore served as a good model system during the method development process [42].

As a first step of the methods development process, the elastic modulus of the PDMS substrate was characterized via compression testing. During initial experiment thin disks, 16mm in diameter, were tested. Elastic modulus values ranging 3-4 MPa were observed, which is significantly higher than the 0.98-2.61 MPa reported in literature given similar processing conditions [36] [67]. As a part of the investigation into these unexpected results, disks of varying areas were compressed. The resulting measured elastic moduli ranged from 3.70 to 1.36 MPa, decreasing with increasing sample area (Figure 4.10a), which is unexpected because modulus is a material property that should be independent of the sample size. More experiments were performed to understand how the testing conditions affected the measured elastic modulus. Figure 4.10b summarizes the effect of lubricating the sample stage and probe before the compression test. Lubricating the sample or increasing the sample diameter leads to a lower observed elastic modulus value. The reason for this discrepancy is the adhesion of the sample to the probe. Lubricating the sample decreases the effects of adhesion and increasing the size of the sample decreases the adhesion effects that occur at the edge. This hypothesis explains the decrease in elastic modulus with increasing area. With a greater sample area, the surface effects at the edge of the sample become less relevant. After discovering this, thicker samples (5-6 mm in thickness) with large areas and lubricated probes were used for future tests.

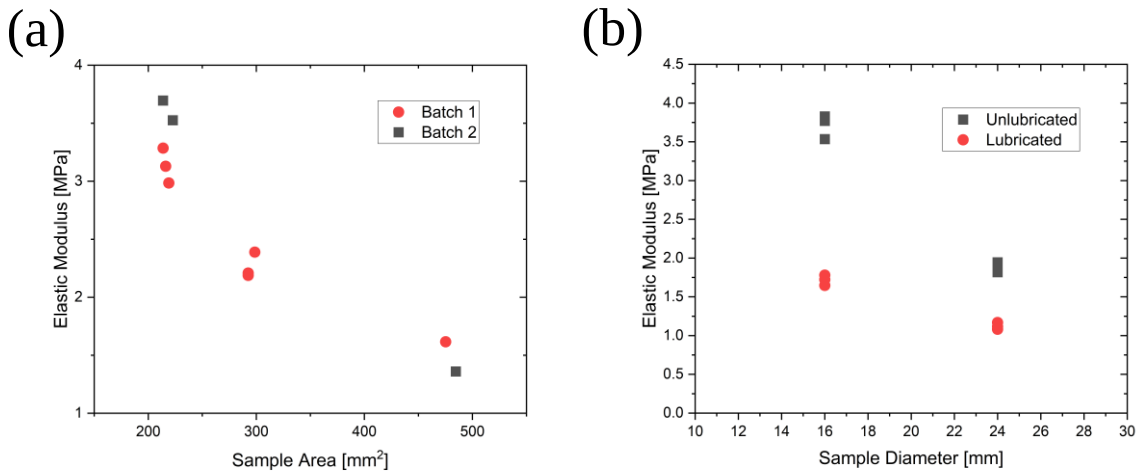


**Figure 4.10** – a) Elastic modulus of the PDMS substrate as a function of sample area. b) Sample lubrication and sample diameter's effect on the measured elastic modulus.

To ensure that compression values were accurate, indentation experiments were also performed, since these experiments assume semi-infinite sample and can be less sensitive to adhesion effects. In an experiment where compression tests were done with thick samples and lubricated probes, the compression tests gave an elastic modulus of 1.88±0.06 MPa, and the indentation test gave an elastic modulus of 1.75±0.99 MPa. These results confirm the accuracy of the compression test. For future experiments, compression was used due to its higher precision and simplicity.

After confirming that accurate elastic modulus for the PDMS substrate could be characterized, wrinkling experiments on polystyrene thin films (N = 6), ranging in 90 to 160 nm in thickness, were performed. As can be seen in Figure 4.11b, the expected characteristic wrinkling pattern was observed for the polystyrene films. The plane-strain elastic modulus was determined to be 4.608±0.439 GPa. This value was consistent with previous literature, which reported values of 4.38-5.00 GPa as summarized in Table 4.1.

**Table 4.3 -** The plane-strain elastic modulus of polystyrene thin films determined by surface wrinkling

| Source | PS MW [kg/mol] | $\bar{E}_f$ [GPa] |
|---|---|---|
| This work | 300 | 4.61 |
| Chung, et. al. [36] | 280 | 4.38 |
| Lee, et. al. [37] | 654 | 5.00 |

4.2.2. Wrinkling of Cellulose Acetate Butyrate Thin Films

Following accurate determination of the modulus of polystyrene via surface wrinkling, the modulus of pristine CAB films was investigated. Early experiments indicated poor adhesion between the CAB films and the PDMS substrate. Films often had visible regions of delamination and surface wrinkles only appeared in small veins rather than uniformly across the sample (Figure 4.11a). The adhesion issues were likely caused by the difference in hydrophobicity of the PDMS substrate, which is relatively hydrophobic, and CAB, which is relatively hydrophilic. To tune the hydrophilicity of the PDMS, UV-ozone and hydrochloric acid treatment were attempted, but with no success. Instead, a two-layer composite system used in a paper by Dr. Adam Nolte was used [35].

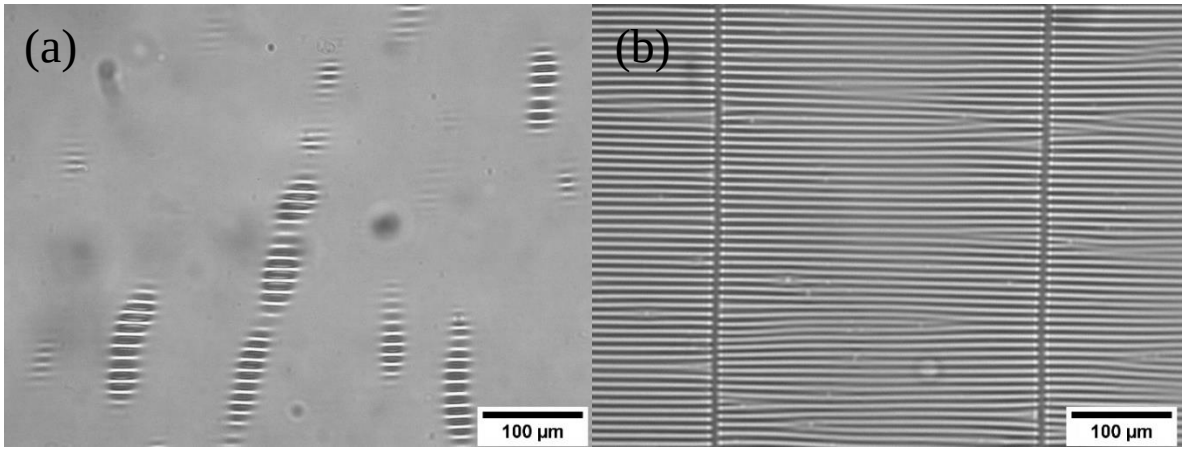


**Figure 4.11 -** a) An example of poor adhesion b) An example of good adhesion with a polystyrene interlayer.

A two-layer composite system with a polystyrene interlayer (~90 nm in thickness) led to much better adhesion with clear and defined wrinkles (Figure 4.11b). Using the interlayer

technique, elastic modulus data were measured for CAB thin films at varying thicknesses and is plotted in Figure 4.12. The data shows a clear decrease in the elastic modulus as the film thickness decreases. This is the same trend seen in other studies looking at the elastic modulus of thin films in confinement [36] [37]. There is a clearly defined bulk regime with a constant elastic modulus with a depression in the elastic modulus. This is because, at lower thicknesses, there is less crystallinity and more free volume within the polymer, making the film less stiff. This is reflected in the swelling data as an increase in swelling activity. Confined films are less resistant to geometric changes, whether they are driven by mechanical stress or chemical potential gradients. Confined films have a greater amount of variability in the elastic modulus due to the increasing importance of accurate thickness measurements for thinner films. At 20 nanometers, the impact of a 2 nm deviation in film thickness of the film is significantly greater than at 200 nanometers. While there is significant variability in the confined region, the trend of a modulus depression is apparent.

An asymptotic function was fitted to the data to determine a value for the elastic modulus in the bulk regime. The results of this regression show the bulk plane-strain elastic modulus of our sample was 1.47 ± 0.09 GPa, which corresponds to an elastic modulus of 1.25 ± 0.08 GPa. Qualitatively, the model tracks with the collected data, following the scatter plot of individual measurements very closely. Further residual analysis of the model shows that the variance follows a normal distribution, with the model skewing slightly high (Figure 4.13). This result is plausible, matching previous elastic modulus values for cellulose acetate butyrate from the literature which ranged from 1.03 to 1.71 GPa (Table 4.2). With this model, we can see the cutoff for the bulk to the confined regime is approximately around 45 nm to 70 nm. This cutoff is in a similar spot to other polymer systems [36] [37]. What is notable is that this cutoff is comparable to the cutoff seen in the swelling behavior of the CAB films (Figure 4.4). Films below 50 nm to 60 nm in thickness

have significantly increased swelling behavior. This strengthens our hypothesis that crystallinity is the primary cause of confinement effects observed in semicrystalline polymers. A decrease in crystallinity in the confinement regime would lead to a decrease in the resistance to deformation, whether the driving force is chemical or mechanical. Crystallinity cannot entirely fully explain confinement effects, as amorphous polymers such as polystyrene also display confinement [44]. The confined geometry changes how the polymer is packed, and crystallinity changes are only one of the changes, but these crystallinity changes explain the changes in swelling behavior and elastic modulus.

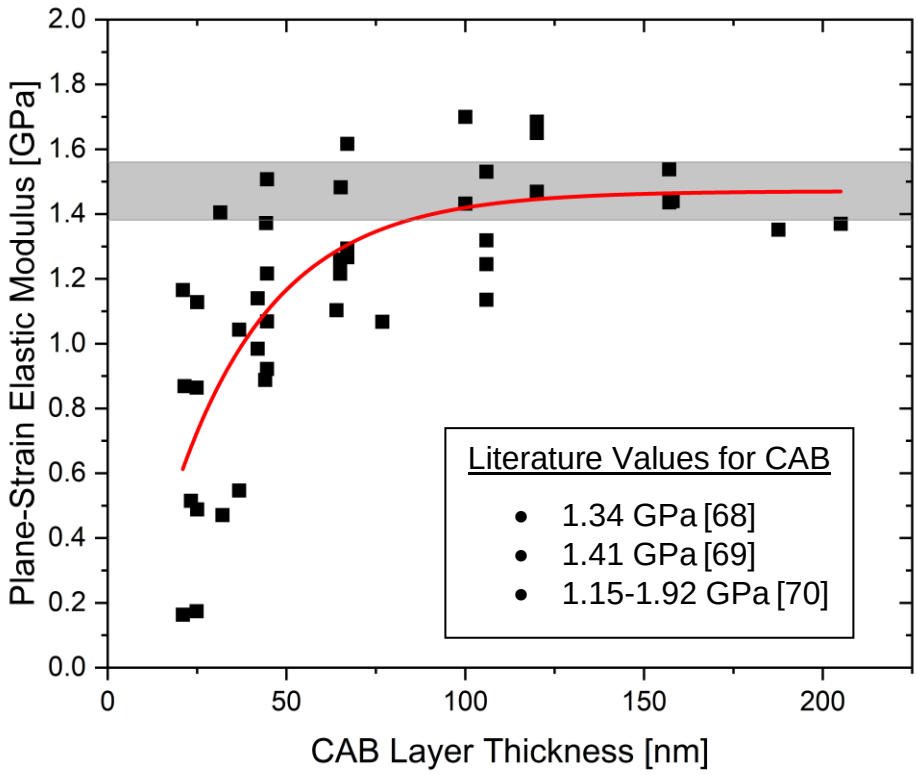


**Figure 4.12 -** The plane-strain elastic modulus of pristine CAB over varying thickness. Each point represents an experiment. The grey bar represents the 95% confidence interval for the bulk regime elastic modulus. The red curve is an asymptotic fit of the data.

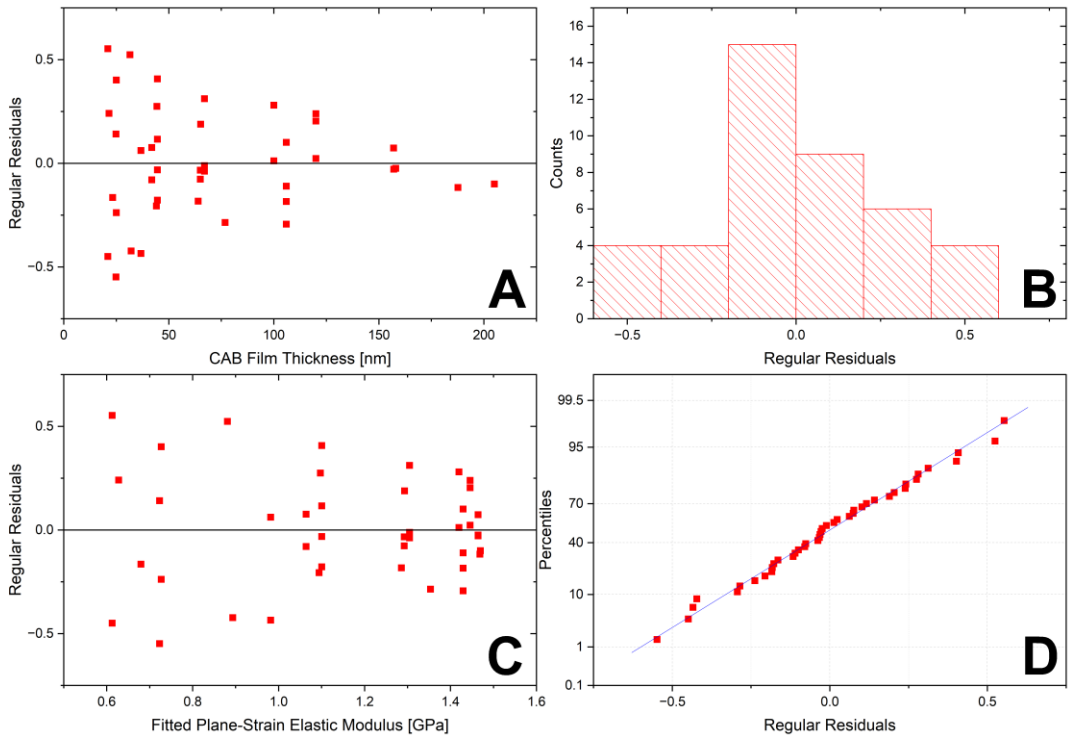


**Figure 4.13 -** Residual statistics for the pristine CAB plane-strain elastic modulus data. A) Regular residuals plotted over the dependent variable showing a greater variance in the lower film thickness regime. B) Regular residuals plotted as a histogram, showing that the variance is normally distributed with the model skewing higher than the data. C) The regular residuals over the model's independent variable, showing a greater variance in the thinner regime. D) Regular residuals across the percentiles, showing that the variance is normally distributed.

**Table 4.4 -** Elastic modulus values for cellulose acetate butyrate found in the literature

| **Source** | **E [GPa]** | **Comments** |
|---|---|---|
| This work | 1.25 | 2% acetyl, 49% butyryl |
| Gindl et al. [68] | 1.20 | SG =1.2 |
| Siqueira et al. [69] | 1.26 | Nanowhiskers, 2% acetyl, 48% butyryl |
| Van de Voorde et al. [70] | 1.03-1.71 | Reference value |

Humidity-based experiments were used to probe the internal plasticization effects of water on the modulus of elasticity. As shown in Figure 4.14, wrinkle wavelength and elastic modulus remained relatively constant with increasing humidity until around 60% relative humidity. With further increasing humidity, the wrinkle wavelength and elastic modulus decreased and had significantly higher variability. Figure 14b shows that thickness changes due to swelling cannot

account for this change because, in the bulk regime, the error caused by thickness changes is greater than the random error. This is not necessarily true in the confined regime or in other polymer systems. The change in elastic modulus is due to the permeation of water into the film, leading to a change in the amount of free volume in the film. A previous study of bulk cellulose acetate samples observed large changes of the mobility of water at around 70% relative humidity [50]. Around this humidity, the mobility of water transitions from a monomolecular level of mobility to a multi-molecular "blob" mobility, where molecules of water begin moving in groups rather than diffusing as single molecules. In this case, water acts as a plasticizer, increasing the free volume within the polymer.

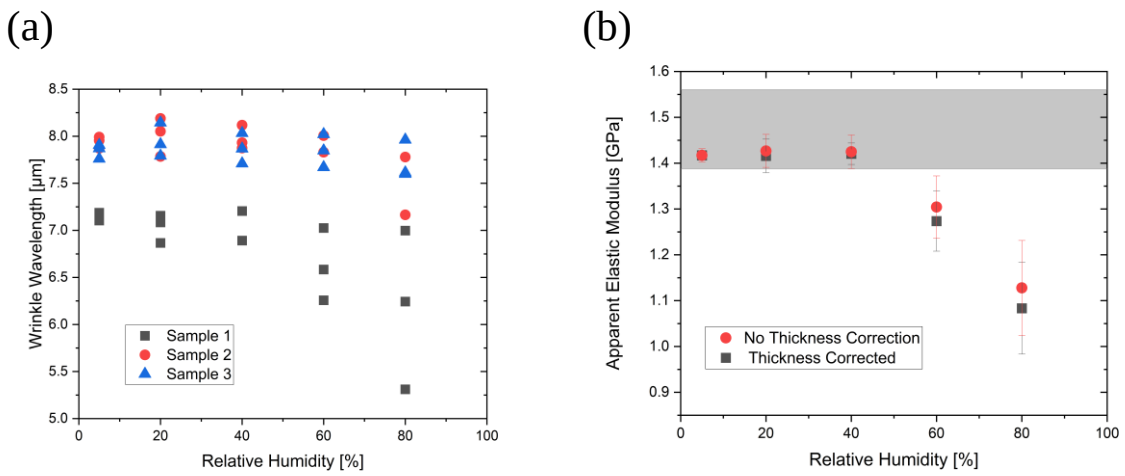


**Figure 4.14 -** a) Wrinkle wavelength of bulk pristine CAB films over varying humidity levels. b) The apparent plane-strain elastic modulus over varying humidity levels. The apparent elastic modulus value is constructed from the wrinkle wavelength measured at a given humidity and all other variables are selected based on processing conditions. Thickness correction used the swelling ratios of soaked CAB films to estimate the thickness at a given humidity level.

The effect of triacetin on the elastic modulus of CAB films was also investigated. The focus was on 10% triacetin because previous literature and our swelling data showed antiplasticization at that level [58]. Figure 4.15a compares modulus values of pristine CAB and triacetin-treated films in both the bulk and confined regimes. Pristine CAB had an elastic modulus of 1.4707±0.09 and

triacetin-treated CAB had an elastic modulus of 1.47±0.14. Figure 4.15b looks at the apparent elastic modulus values in humidity experiments. Triacetin had no effect on the elastic modulus of the CAB films. The increase in elastic modulus at 5% humidity in Figure 4.15b is due to the fewer number of samples used for humidity experiments. The fact that antiplasticization effects are clear in swelling behavior but not mechanical properties provides some insight into the mechanism of antiplasticization in this system. Previous x-ray scattering data has shown that a low level of triacetin treatment does not significantly change the crystallinity of the overall polymer sample [66]. If the crystallinity is not significantly changing, then the mechanical properties stay the same while swelling behavior changes due to the amorphous regions of the polymer relaxing.

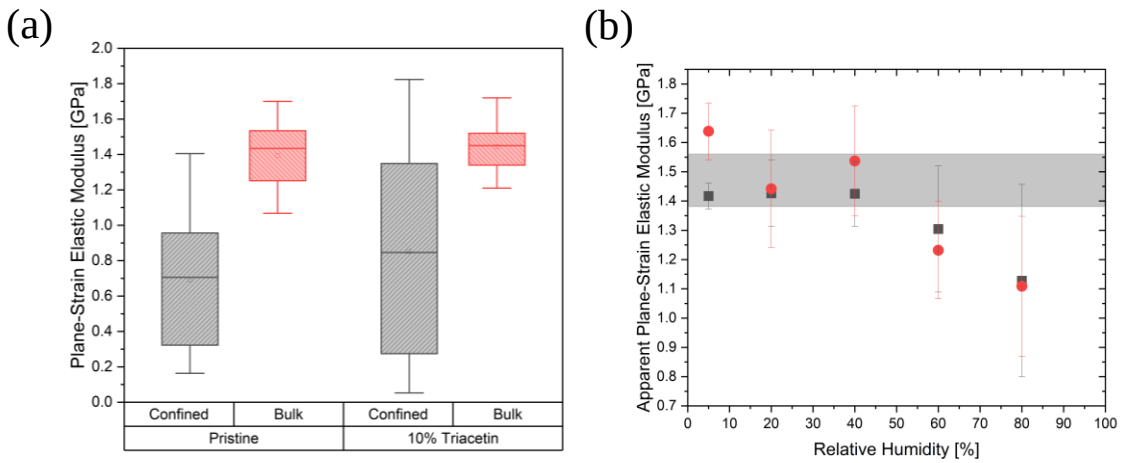


**Figure 4.15 –** a) The plane-strain elastic modulus for pristine and 10% triacetin treated samples compared in the bulk and confined regimes. b) Apparent plane-strain elastic modulus values for both pristine and treated CAB films across multiple humidity levels.

## 5. Conclusions and Further Work

By modifying the casting dope and the parameters of film fabrication, we were able to fabricate films of different thicknesses, elastic moduli, and swelling properties. We demonstrated thin film confinement with a cutoff around 45 to 70 nm. This leads to a depression in elastic modulus and an 11.8% increase in the swelling ratio at high humidity levels. This was correlated to crystallinity data in cellulose triacetate, which shows a decrease in crystallinity in this length

scale [62]. Modifying the films by soaking them lead to a decrease in swelling activity. Triacetin treatment did not effect elastic modulus values but did increase the swelling ratio with triacetin treatments at 20%-40% by weight in the film. At 10% triacetin by weight in the film, antiplasticization was demonstrated by a decrease in the swelling ratio. These changes were correlated to crystallinity data and permeability data showing similar trends [66] [58]. We also documented a depression in elastic modulus with increasing humidity, indicating water functioning as an internal plasticizer. With this information, we believe we can use fundamental polymer physics in novel systems as a simple pre-screen method for developing higher-performance membranes before membrane fabrication. Even so, future work should involve transport property testing. While we believe that the demonstration of this in literature is enough to support the argument, the fabrication of membranes optimized by these experiments and other treatments will further strengthen this as a method to develop higher-performance membranes. Another study to be done should focus on mechanical property characterization on CAB films at higher triacetin contents. This will help confirm our theory as to the mechanism of plasticization and antiplasticization. A deeper understanding of these phenomena will allow for significantly greater control over the design of membrane materials.

**References**

[1] W. Wu, H. R. Maier, G. C. Dandy, M. Arora and A. Castelletti, "The changing nature of the water–energy nexus in urban water supply systems: a critical review of changes and responses," *Journal of Water and Climate Change,* vol. 11, no. 4, pp. 1095-1122, 2020.

[2] Baker, Membrane Technology and Applications, West Sussex: Wiley, 2012.

[3] M. K. Shahid, A. Kashif, P. Pathak, Y. Choi and P. R. Rout, Clean Energy and Resource Recovery, Elsevier, 2022.

[4] S. M. Mrayed, P. Sanciolo, L. Zou and G. Lesie, "An alternative membrane treatment process to produce low-salt and high-nutrient recycled water suitable for irrigation purposes," *Desalination,* vol. 274, no. 1-3, pp. 144-149, 2011.

[5] K. P. Lee, T. C. Arnot and D. Mattia, "A review of reverse osmosis membrane materials for desalination - Development to date and future potential," *Journal of Membrane Science,* vol. 370, no. 1-2, pp. 1-22, 2011.

[6] H. Nassrullah, S. Anis and R. Hashaikeh, "Energy for desalination: A state-of-the-art review," *Desalination,* vol. 491, no. June, 2020.

[7] G. C. Flemming, "Reverse osmosis membrane biofouling," *Experimental Thermal Fluid Science,* vol. 14, pp. 382-391, 1997.

[8] C. S. Ong, P. S. Goh, W. J. Lau, N. Misdan and A. F. Ismail, "Nanomaterials for biofouling and scaling mitigation of thin film composite membrane: A review," *Desalination,* vol. 393, pp. 2-15, 2016.

[9] H. C. Flemming and G. Schaule, "Biofouling on membranes - a microbiological approach," *Desalination,* vol. 70, pp. 95-119, 1988.

[10] T. R. Garrett, M. Bhakoo and Z. Zhang, "Bacterial adhesion and biofilms on surfaces," *Progress in Natural Science,* vol. 18, no. 9, pp. 1049-1056, 2008.

[11] P. R. Rout, T. C. Zhang, P. Bhunia and R. Y. Surampalli, "Treatment technologies for emerging contaminants in wastewater treatment plants: A review," *Science of the Total Environment,* vol. 753, p. 141990, 2021.

[12] R. L. Riley, H. K. Lonsdale, C. R. Lyons and U. Merton, "Preparation of Ultrathin Reverse Osmosis Membranes and the Attainment of Theoretical Salt Rejection," *Journal of Applied Polymer Science,* vol. 11, no. 11, pp. 2143-2158, 1967.

[13] R. Lu, X. Zhang, H. Wang, R. M. Briber and H. Wang, "Amorphous cellulose thin films," *Cellulose,* vol. 27, no. 6, pp. 2959-2965, 2020.

[14] H. Nguyen, M. Wang, M.-Y. Hsiao, K. Nagai, Y. Ding and H. Lin, "Suppression of crystallization in thin films of cellulose diacetate and its effect on CO2/CH4 separation properties," *Journal of Membrane Science,* vol. 586, pp. 7-14, 2019.

[15] J. Bitter, "Effect of Crystallinity and Swelling on the Permeability and Selectivity of Polymer Membranes," *Desalination,* vol. 51, pp. 19-35, 1984.

[16] B. S. Lalia, V. Kochkodan, R. Hashaikeh and N. Hilal, "A review on membrane fabrication: Structure, properties and performance relationship," *Desalination,* vol. 326, pp. 77-95, 2013.

[17] W. Lau, A. Ismail, N. Misdan and M. Kassim, "A recent progress in thin film composite membrane: A review," *Desalination,* vol. 287, pp. 190-199, 2012.

[18] H. K. Lonsdale, U. Merten and R. L. Riley, "Transport Properties of Cellulose Acetate Osmotic Membranes," *Journal of Applied Polymer Science,* vol. 9, pp. 1341-1362, 1965.

[19] J. A. Jr., P. M. Kosaka and D. F. S. Petri, "Characteristics of thin cellulose ester films spin-coated from acetone and ethyl acetate solutions," *Cellulose,* vol. 15, no. 4, pp. 527-535, 2008.

[20] J. S. Gardner, J. O. Walker and J. D. Lamb, "Permeability and durability effects of cellulose polymer variation in polymer inclusion membranes," *Journal of Membrane Science,* vol. 229, no. 1-2, pp. 87-93, 2004.

[21] J. E. Cadotte, R. J. Petersen, R. E. Larson and E. E. Erickson, "A new thin-film composite seawater reverse osmosis membrane," *Desalination,* vol. 32, pp. 25-31, 1980.

[22] P. S. Goh and A. F. Ismail, "Chemically functionalized polyamide thin film composite membranes: The art of chemistry," *Desalination,* vol. 495, no. June, p. 114655, 2020.

[23] J. Zhu, J. Hou, Y. Zhang, M. Tian, T. He, J. Liu and V. Chen, "Polymeric antimicrobial membranes enabled by nanomaterials for water treatment," *Journal of Membrane Science,* vol. 550, pp. 173-197, 2018.

[24] N. M. Mazlan, P. Marchetti, H. Maples, B. Gu, S. Karan, A. Bismarck and A. G. Livingston, "Organic fouling behavior of structurally and chemically different forward osmosis membranes - A study of cellulose triacetate and thin film composite membranes," *Journal of Membrane Science,* vol. 520, pp. 247-261, 2016.

[25] B. Zhang, X. Song, L. D. Nghiem, G. Li and W. Luo, "Osmotic membrane bioreactors for wastewater reuse: Performance comparison between cellulose triacetate and polyamide thin film composite membranes," *Journal of Membrane Science,* vol. 539, pp. 383-391, 2017.

[26] R. Petersen and J. Cadotte, "Thin film composite reverse osmosis membranes," in *Handbook of Industrial Membrane Technology,* Park Ridge, NJ, Noyes Publications, 1990, pp. 307-348.

[27] J.-H. Lee, J. Y. Chung, E. P. Chan and C. M. Stafford, "Correlating chlorine-induced changes in mechanical properties to performance in polyamide-based thin film composite membranes," *Journal of Membrane Science,* vol. 433, no. April, pp. 72-79, 2013.

[28] X. Lu, X. Feng, Y. Yang, J. Jiang, W. Cheng, C. Liu, M. Gopinadhan, C. O. Osuji and J. M. &. M. Elimelech, "Tuning the permselectivity of polymeric desalination membranes via control of polymer crystallite size," *Nature Communications,* pp. 3-9, 2019.

[29] C. M. Stafford, "A buckling-based metrology for measuring the elastic moduli of polymeric thin films," *Nature Materials,* vol. 3, no. August, pp. 545-550, 2004.

[30] H. We and T. G. M. v. d. Ven, "AFM-Based Single Molecule Force Spectroscopy of Polymer Chains: Theoretical Models and Applications," *Applied Spectroscopy Reviews,* vol. 43, no. 2, pp. 111-133, 2008.

[31] D. M. Ebenstein and K. J. Wahl, "A comparison of JKR-based methods to analyze quasi-static and dynamic indentation force curves," *Journal of Colloid and Interface Science,* vol. 298, no. 2, pp. 652-662, 2006.

[32] J. Y. Chung, A. J. Nolte and C. M. Stafford, "Surface Wrinkling: A Versatile Platform for Measuring Thin-Film Properties," *Advanced Materials,* vol. 23, no. 3, pp. 349-368, 2011.

[33] J. M. Torres, C. M. Stafford and B. D. Vogt, "Manipulation of the Elastic Modulus of Polymers at the Nanoscale: Influence of UV Ozone Cross-Linking and Plasticizer," *American Chemical Society Nano,* vol. 4, no. 9, pp. 5357-5365, 2010.

[34] A. J. Nolte, N. D. Treat, R. E. Cohen and M. F. Rubner, "Effect of Relative Humidity on the Young's Modulus of Polyelectrolyte Multilayer Films and Related Nonionic Polymers," *Macromolecules,* vol. 41, pp. 5793-5798, 2008.

[35] A. J. Nolte, "A Two-Plate Buckling Technique for Thin Film Modulus Measurements: Applications to Polyelectrolyte Multilayers," *Macromolecules,* vol. 39, no. 14, pp. 4841-4847, 2006.

[36] J. Y. e. a. Chung, "Stiffness, Strength, and Ductility of Nanoscale Thin Films and Membranes: A Combined Wrinkling-Cracking Methodology," *ACS Nano Letters,* vol. 11, no. 8, pp. 3361-3365, 2011.

[37] J. H. Lee, "Effect of Confinement on Stiffness and Fracture of Thin Amorphous Polymer Films," *ACS Macro Letters,* vol. 1, no. 122-126, p. 1, 2012.

[38] J. Forrest, K. Dalnoki-Veress, J. R. Stevens and J. Dutcher, "Effect of Free Surfaces on the Glass Transition Temperature of Thin Polymer Films," *Physical Review Letters,* vol. 77, no. 10, pp. 8-11, 1996.

[39] J. Forrest and J. Dutcher, "Interface and chain confinement effects on the glass transition temperature of thin polymer films," *Physical Review E,* vol. 56, no. 5, pp. 5705-5716, 1997.

[40] C. Ellison, M. Mundra and J. Torkelson, "Impacts of Polystyrene Molecular Weight and Modification to the Repeat Unit Structure on the Glass Transition - Nanoconfinement and the Cooperativity Length Scale," *Macromolecules,* vol. 5, no. 1767-1778, p. 38, 2005.

[41] B. D. Vogt, "Mechanical and Viscoelastic Properties of Confined Amorphous Polymers," *Journal of Polymer Science: Polymer Physics,* vol. 56, no. 1, pp. 9-30, 2017.

[42] J. A. Forrest, "A decade of dynamics in thin films of polystyrene: Where are we now?," *The European Physical Journal E,* vol. 8, pp. 261-266, 2002.

[43] M. Alcoutlabi and G. B. McKenna, "Effects of confinement on the material behaviour at the nanometre size scale," *Journal of Physics: Condensed Matter,* vol. 17, pp. 461-524, 2005.

[44] E. P. Chan, A. P. Young, J.-H. Lee and C. M. Stafford, "Swelling of Ultrathin Molecular Layer-by-Layer Polyamide Water Desalination Membranes," *Journal of Polymer Science: Polymer Physics,* vol. 51, no. 22, pp. 1647-1655, 2013.

[45] J. M. Torres, C. Wang, E. B. Coughlin, J. P. Bishop, R. A. Register, R. A. Rigglemann, C. M. Stafford and B. D. Vogt, "Influence of chain stiffness on thermal and mechanical properties of polymer thin films," *Macromolecules,* vol. 44, no. 22, pp. 9040-9045, 2011.

[46] W. D. Mulhearn, V. P. Oleshko and C. M. Stafford, "Thickness-Dependent Permeance of Molecular Layer-By-Layer Polyamide Membranes," National Institute of Standards Technology, Materials Science and Engineering Division, Gaithersburg, 2021.

[47] P. J. Flory and J. R. Jr., "Statistical Mechanics of Cross-Linked Polymer Networks," *Journal of Chemical Physics,* vol. 11, p. 521, 1943.

[48] E. Chan and S. Lee, "Thickness-dependent swelling of molecular layer-by-layer polyamide nanomembranes," *Journal of Polymer Science Part B: Polymer Physics,* vol. 55, no. 5, pp. 412-417, 2017.

[49] J. Wong, F. Rehfeldt, P. Hanni and e. a., "Swelling behavior of polyelectrolyte multilayers in saturated water vapor," *Macromolecules,* vol. 37, no. 19, pp. 7285-7289, 2004.

[50] G. Banik and I. Bruckle, "Principles of Water Absorption and Desorption in Cellulosic Materials," *Resaurator,* vol. 31, pp. 164-177, 2010.

[51] R. M. Nelson, "A Model For Sorption of Water Vapor By Cellulosic Materials," *Wood and Fiber Science,* vol. 1, no. 8-22, p. 15, 1983.

[52] J. Nichols, "Nitrocellulose and Camphor," *Journal of Physical Chemistry,* vol. 28, pp. 769-771, 1923.

[53] S. Brous and W. Semon, "Koroseal: A New Plastic: Some Properties and Uses," *Industrial Engineering Chemistry,* vol. 27, pp. 667-672, 1935.

[54] B. Wadey, "Plasticizers," in *Encyclopedia of Physical Science and Technology,* Academic Press, 2003, pp. 441-456.

[55] N. Kinjo and T. Nakagawa, "Antiplasticization in the Slightly Plasticized Polyvinyl Chloride," *Journal of the Society of Material Science Japan,* vol. 22, pp. 462-465, 1973.

[56] J. S. Vrentas, J. L. Duda and H. Ling, "Antiplasticization and Volumetric Behavior in Glassy Polymers," *Macromolecules,* vol. 21, no. 5, pp. 1470-1475, 1988.

[57] L. Mascia, Y. Kouparitas, D. Nocita and X. Bao, "Antiplasticization of Polymer Materials: Structural Aspects and Effects on Mechanical and Diffusion-Controlled Properties," *Polymers,* vol. 769, no. 12, pp. 1-37, 2020.

[58] J.-H. Guo, "Effects of Plasticizers on Water Permeation and Mechanical Properties of Cellulose Acetate: Antiplasticization in Slightly Plasticized Polymer Film," *Drug Development and Industrial Pharmacy,* vol. 19, no. 13, pp. 1541-1555, 1993.

[59] H. Frey and H. R. Kahn, Handbook of Thin-Film Technology, Berlin: Springer, 2015.

[60] H. G. Tompkins and J. N. Hilfiker, Spectroscopic Ellipsometry: Practical Application to Thin Film Characterization, New York City: Momentum Press, 2016.

[61] C. M. Stafford, S. Guo, C. Harrison and M. Y. M. Chiang, "Combinatorial and high-throughput measurements of the modulus of thin polymer films," *Review of Scientific Instruments,* vol. 76, p. 062207, 2005.

[62] H. Nguyen, M.-Y. Hsiao, K. Nagai and H. Lin, "Suppressed crystallization and enhanced gas permeability in thin films of cellulose acetate blends," *Polymer,* vol. 205, p. 122790, 2020.

[63] D. Perera, S. Nataraj, N. Thomson, S. H. A. Sepe, U. Steiner, H. Qiblawey and E. Sivaniah, "Room-temperature development of thin film composite reverse osmosis membranes from cellulose acetate with antibacterial properties," *Journal of Membrane Science,* vol. 453, pp. 212-220, 2014.

[64] C. Fordyce and L. Meyer, "Plasticizers for Cellulose Acetate and Cellulose Acetate Butyrate," *Industrial and Engineering Chemistry,* vol. 32, no. 8, pp. 1053-1060, 1940.

[65] R. Navarro, M. Pérez Perrino, M. Gómez Tardajos and H. Reinecke, "Phthalate Plasticizers Covalently Bound to PVC: Plasticization with," *Macromolecules,* vol. 43, pp. 2377-2381, 2010.

[66] C. Bao, *Cellulose acetate / plasticizer systems : structure, morphology and dynamics,* Lyon: Université Claude Bernard, 2015.

[67] Z. Wang, A. A. Volinsky and N. D. Gallant, "Crosslinking Effect on Polydimethylsiloxane Elastic Modulus Measured by Custom-Built Compression Instrument," *Journal of Applied Polymer Science,* vol. 131, no. 22, p. 41050, 2014.

[68] W. Grindl and J. Keckes, "Tensile properties of cellulose acetate butyrate composites reinforced with bacterial cellulose," *Composites Science and Technology,* vol. 64, pp. 2407-2413, 2004.

[69] G. Siqueira, A. P. Mathew and K. Oksman, "Processing of cellulose nanowhiskers/cellulose acetate butyrate nanocomposites using sol-gel process to facilitate dispersion," *Composites Science and Technology,* vol. 71, no. 16, pp. 1886-1892, 2011.

[70] M. Van de Voorde and G. Pluym, "Radiation Damage of Materials," CERN, Geneva, 1966.

[71] A. Matin, F. Rahman, H. Z. Shafi and S. M. Zubair, "Scaling of reverse osmosis membranes used in water desalination: Phenomena, impact, and control; future directions," *Desalination,* vol. 455, no. September 2018, pp. 135-157, 2019.

[72] O. K. C. Tsui and T. P. Russell, "Effect of Interfacial Interactions on the Glass Transition of Polymer Thin Films," *Macromolecules,* vol. 34, pp. 5535-5539, 2001.

[73] M. Smyda and S. Harvey, "The Entropic Cost of Polymer Confinement," *The Journal of Physical Chemistry B,* vol. 116, pp. 10928-10934, 2012.

[74] Polymer Database, "CELLULOSE ACETATE BUTYRATE," 2015. [Online]. Available: https://polymerdatabase.com/Polymer%20Brands/CAB.html. [Accessed September 2022].

[75] P. C. Painter and S. L. Shenoy, "A simple model for the swelling of polymer networks," *The Journal of Chemical Physics,* vol. 99, no. 2, pp. 1409-1418, 1993.

[76] R. I. Quintero, M. J. Galotta, F. Rodriguez and A. Guarda, "Preparation and Characterization of Cellulose Acetate Butyrate/Organoclay Nanocomposites Produced by Extrusion," *Packaging Technology and Science,* vol. 27, no. 6, pp. 495-507, 2013.

[77] D. J. A. Jr. and P. M. Kosaka, "Characteristics of thin cellulose ester films spin-coated from acetone and ethyl acetate solutions," *Drug Development and Industrial Pharmacy,* vol. 19, no. 13, pp. 1541-1555, 1993.